JAERI-M
83-082

TEMPERATURE DISTRIBUTION MEASUREMENT IN THE HOT GAS DUCT OF HENDEL

(RESULTS OF TESTS, NO.1 CYCLE AND NO.2 CYCLE OPERATIONS)

(February 1982~October 1982)

June 1983

Kazuhiko KUNITOMI, Ikuo IOKA, Kozi UMENISHI, Makoto HISHIDA,
Toshiyuki TANAKA, Hiroaki SHIMOMURA and Konomo SANOKAWA

日本原子力研究所
Japan Atomic Energy Research Institute

JAERI-Mレポートは，日本原子力研究所が不定期に公刊している研究報告書です。
入手の問合わせは，日本原子力研究所技術情報部情報資料課（〒319-11茨城県那珂郡東海村）あて，お申しこしください。なお，このほかに財団法人原子力弘済会資料センター（〒319-11茨城県那珂郡東海村日本原子力研究所内）で複写による実費頒布をおこなっております。

JAERI-M reports are issued irregularly.
Inquiries about availability of the reports should be addressed to Information Section, Division of Technical Information, Japan Atomic Energy Research Institute, Tokai-mura, Naka-gun, Ibaraki-ken 319-11, Japan.

編集兼発行　日本原子力研究所
印　　刷　いばらき印刷㈱

JAERI-M 83-082

Temperature distribution measurement in the hot gas duct of HENDEL (Results of tests, NO.1 cycle and NO.2 cycle operations) (February 1982 ∿ October 1982)

Kazuhiko KUNITOMI, Ikuo IOKA, Kozi UMENISHI
Makoto HISHIDA, Toshiyuki TANAKA, Hiroaki SHIMOMURA
and Konomo Sanokawa

Department of High Temperature Engineering
Tokai Research Establishment, JAERI
(Received May 17, 1983)

The HENDEL (Helium Engineering Demonstration Loop) which was completed on March, 1982, has been operated 3 times so far, including a test operation when it was handed over to JAERI. In the main part of HENDEL which is called a Mother + Adapter (M+A) loop, a hot gas duct through which helium gas of 1000°C, 40 atm, 4kg/s flows is installed.

This report deals with the measurement and evaluation of temperature distribution of the hot gas duct. The maximum surface temperature of the hot gas duct was 230°C, which is low enough, compared with an allowable design temperature of 350°C. The effective thermal conductivity of the insulation inside the hot gas duct was found to be 0.40 - 0.49 kcal/mh°C.

Keywords; Hot Gas Duct, Thermal Insulation, HTGR, Helium Engineering Demonstration Loop, Temperature Distribution, Performance

---

The most part of this report was presented at the 3rd task manager meeting for components under the contract between KFA, Jülich, and JAERI, which was held at JAERI, Tokai, in December 1982.

JAERI－M 83－082

HENDEL高温配管温度分布の測定

日本原子力研究所東海研究所高温工学部
国富　一彦・井岡　郁夫・梅西　浩二・菱田　　誠
田中　利幸・下村　寛昭・佐野川好母

（1983年5月17日受理）

HENDEL（Helium Engineering Demonstration Loop）は，1982年3月に完成し，現在までに検収運転を含めて3回の試験運転を行った。HENDELの本体部であるマザー＋アダプターループ（M＋Aループ）には，温度1000℃，圧力40気圧，最大流量4 kg/sのヘリウムガスが流れる高温配管が設置されている。

本報告書は，この高温配管の温度分布計測結果について述べたものである。この結果，高温配管表面温度は最大230℃であり，設計温度の350℃を十分下回るものであった。また，高温配管断熱材の有効熱伝導率は，0.40～0.49 kcal/mh℃であった。

（注）　本報告は，原研東海研究所で1982年12月に行われた，原研―ユーリッヒ研との第3回コンポーネント・タスクミーティングに提出されたものである。

CONTENTS

目　　次

1. Outline of the Helium Engineering Demonstration Loop (HENDEL)

Prior to the construction of the experimental VHTR, it is required to establish engineering backgrounds for utilizing helium gas as reactor coolant and to confirm safety and feasibility of both reactor core structures and high temperature components.

For these purposes, HENDEL is designed to test various mock-up components of the reactor, such as fuel stack, control rod, core structures, core barrel, hot gas ducts, valves, intermediate heat exchanger, etc.

Figure 1 shows a flow diagram of HENDEL. HENDEL consists of Mother(M), Adapter(A) and test sections (T1-T4). Mother and Adapter (M+A) is designed to supply helium gas to the test sections with simulated VHTR operation conditions of pressure, temperature, flow rate, etc.

The construction of M+A was completed in February 1982. Design and construction of the test sections are now under way.

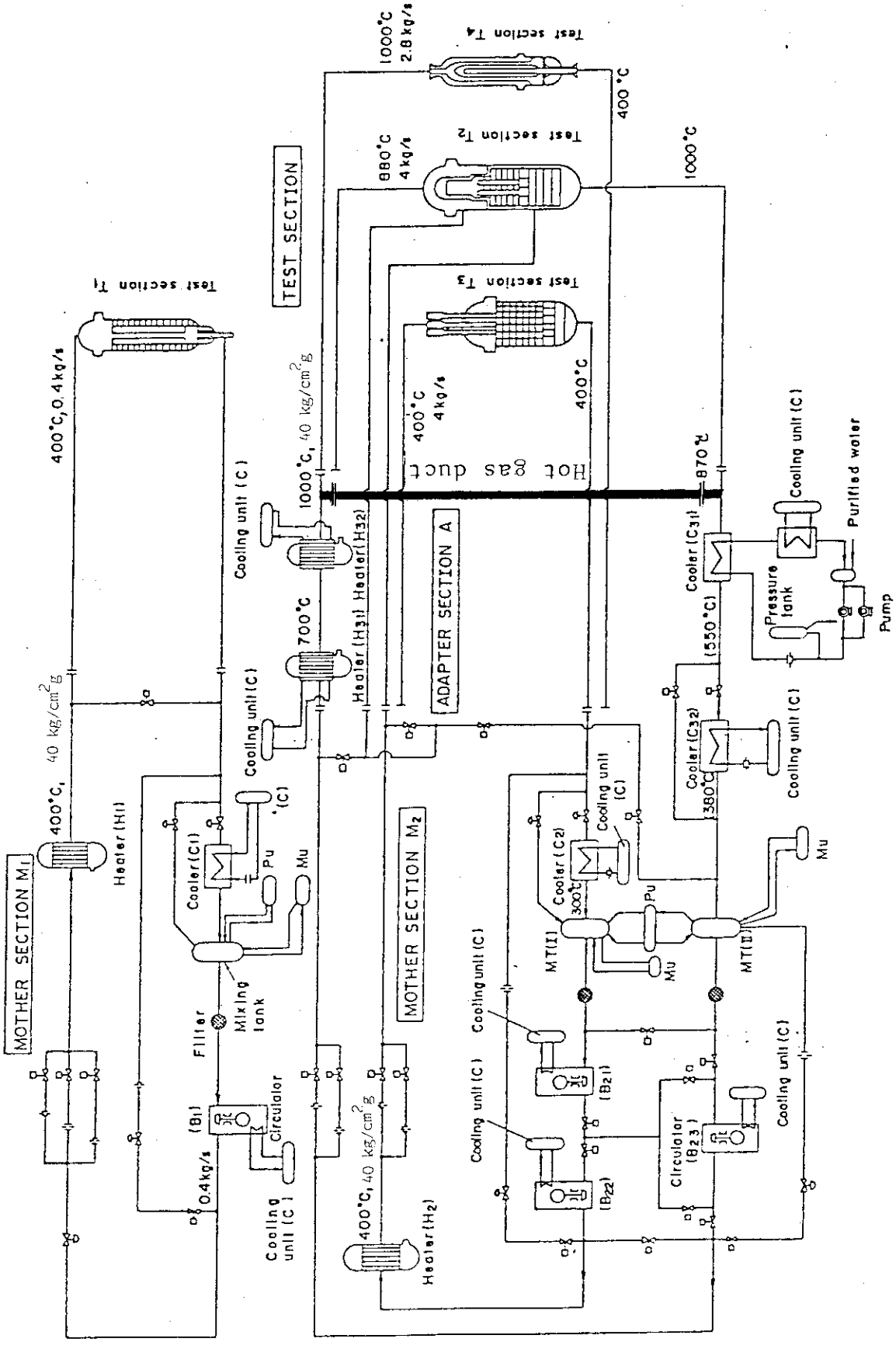

Fig.1 HENDEL main loop flow sheet

2. Operating history of the M+A loop

M+A loop has been operated three times since February 1982. The test operation was performed from February 24 to March 30, NO.1 test cycle from June 21 to July 10, and NO.2 test cycle from September 20 to October 24.

Figure 2.1 shows the operating history of M+A loop.

Tables 2.1∿2.3 show the total operating time in each run. Accumulated operating time is 365 hours at the helium gas temperature 800∿1000°C. During the course of operation, various data were obtained to confirm the capacity of heaters or coolers and the ability of suppling helium gas to the test sections with simulated operating conditions. As for the hot gas duct, transporting 1000°C helium gas from heaters to coolers, temperature distribution in the insulation layer, surface temperature of the pressure tube, heat flux, etc. were measured.

The measured data are tabulated in Appendix 1.

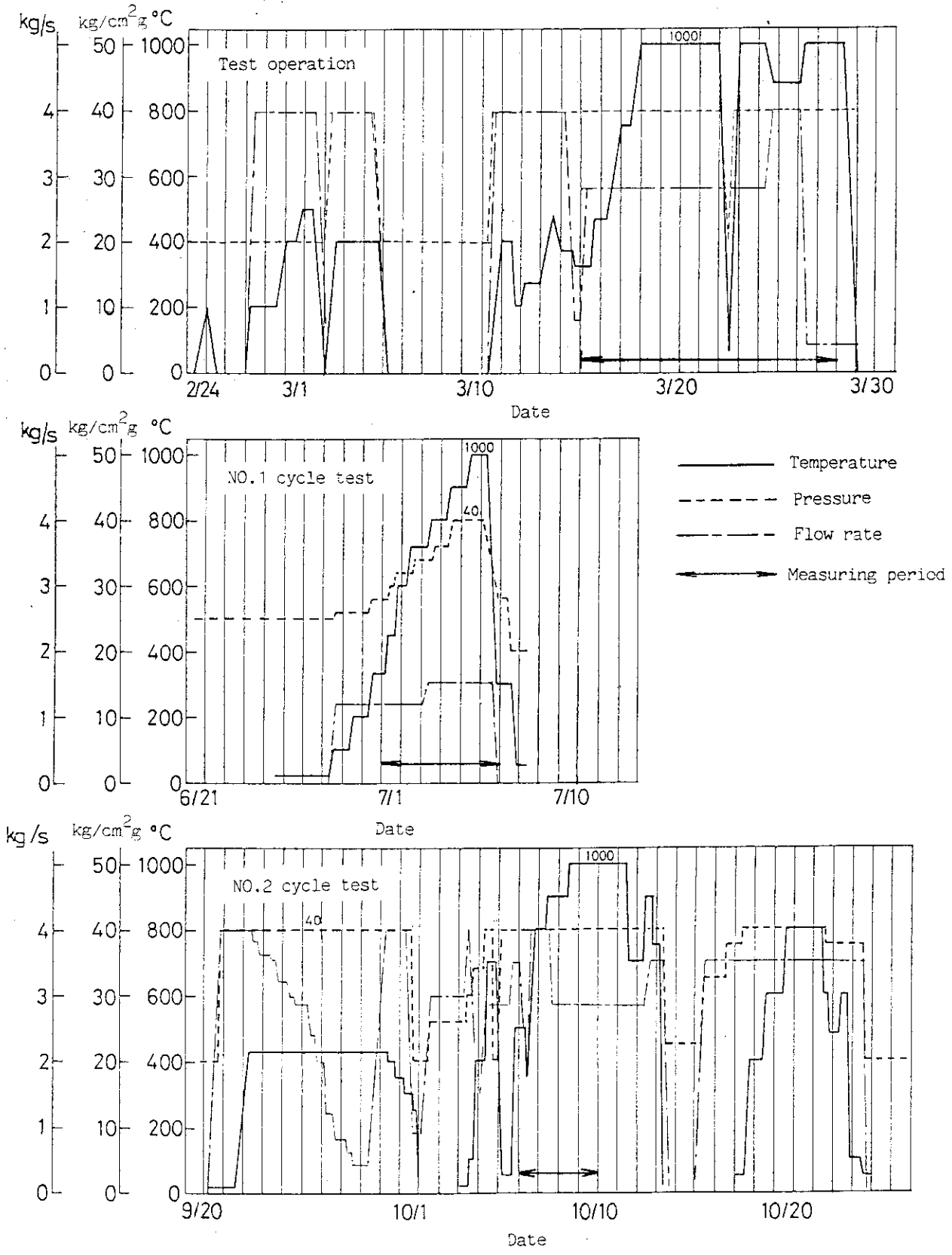

Fig.2.1 Operating history of M+A loop

Table 2.1 Test operation (2/24-3/31)

	M1 Loop	M+A Loop
~ 300°C	20 hr	45 hr
301 ~ 450°C	230 hr	240 hr
451 ~ 800°C	--	50 hr
801 ~ 1000°C	--	215 hr
total	250 hr	550 hr

Table 2.2 NO.1 Cycle (6/21-7/10)

	M1 Loop	M+A Loop
~ 300°C	40 hr	50 hr
301 ~ 450°C	310 hr	20 hr
451 ~ 800°C	--	70 hr
801 ~ 1000°C	--	50 hr
total	350 hr	190 hr

Table 2.3 NO.2 Cycle (9/20-10/26)

	M1 Loop	M+A Loop
~ 300°C	--	450 hr
301 ~ 450°C	--	250 hr
451 ~ 800°C	--	215 hr
801 ~ 1000°C	--	100 hr
total	--	1015 hr

3. Specifications of the HENDEL hot gas duct

Table 3.1 shows specifications of the HENDEL hot gas duct which is placed between the heater H32 and the cooler C31.

Figure 3.1 shows a layout of the hot gas duct. This hot gas duct is about 14m long jointed by three flanges.

Figures 3.2∿3.3 indicate a cross section of the hot gas duct and a part of its cross section in detail. There are three layers of fibre insulation between the pressure tube and the liner. The total thickness of the insulation layer is about 120mm. This insulation is Kaowool made of SiO_2 and Al_2O_3. The packed density of the outer, middle and inner insulations are respectively 250 kg/m^3, 200 kg/m^3 and 200 kg/m^3. There are stainless steel foils inserted between each insulation in order to prevent free convection. In the axial direction, V-shape end-pieces are installed to prevent by-pass flow. Axial thermal expansion difference between the pressure tube and the liner is absorbed by a slide-joint at each end of the liner. As for the bend tubes, there are another slide pins supporting the bend liner with a slide-joint. Radial thermal expansion difference between the pressure tube and the liner is absorbed by the studs which support the liner. Each stud is composed of two parts. One is welded to the pressure tube, and the other to the liner. Two parts are jointed by a pin. Around the pin, there are gaps to absorb the difference of the thermal expansions.

Table 3.1 Specifications of the HENDEL hot gas duct

Items	Hot Gas Duct NO.1
Form	Fibre Insulation
Length	H32 - C31 14m
Gas Temperature	H32 Outlet 1000°C C31 Inlet 990°C
Gas Preessure	40 kg/cm^{2}g
Design Temperature	350°C (Pressure Tube)
Design Pressure	45 kg/cm^{2}g
Dimension	Pressure Tube 660.4 O/D X 22 t Liner 355.6 O/D X 6 t
Material	Pressure Tube SB 42 Liner Hastelloy X Insulation Kaowool
Method of Cooling	Natural Cooling
Packed Density	(outer) 250 kg/m^3 (inner, middle) 200 kg/m^3

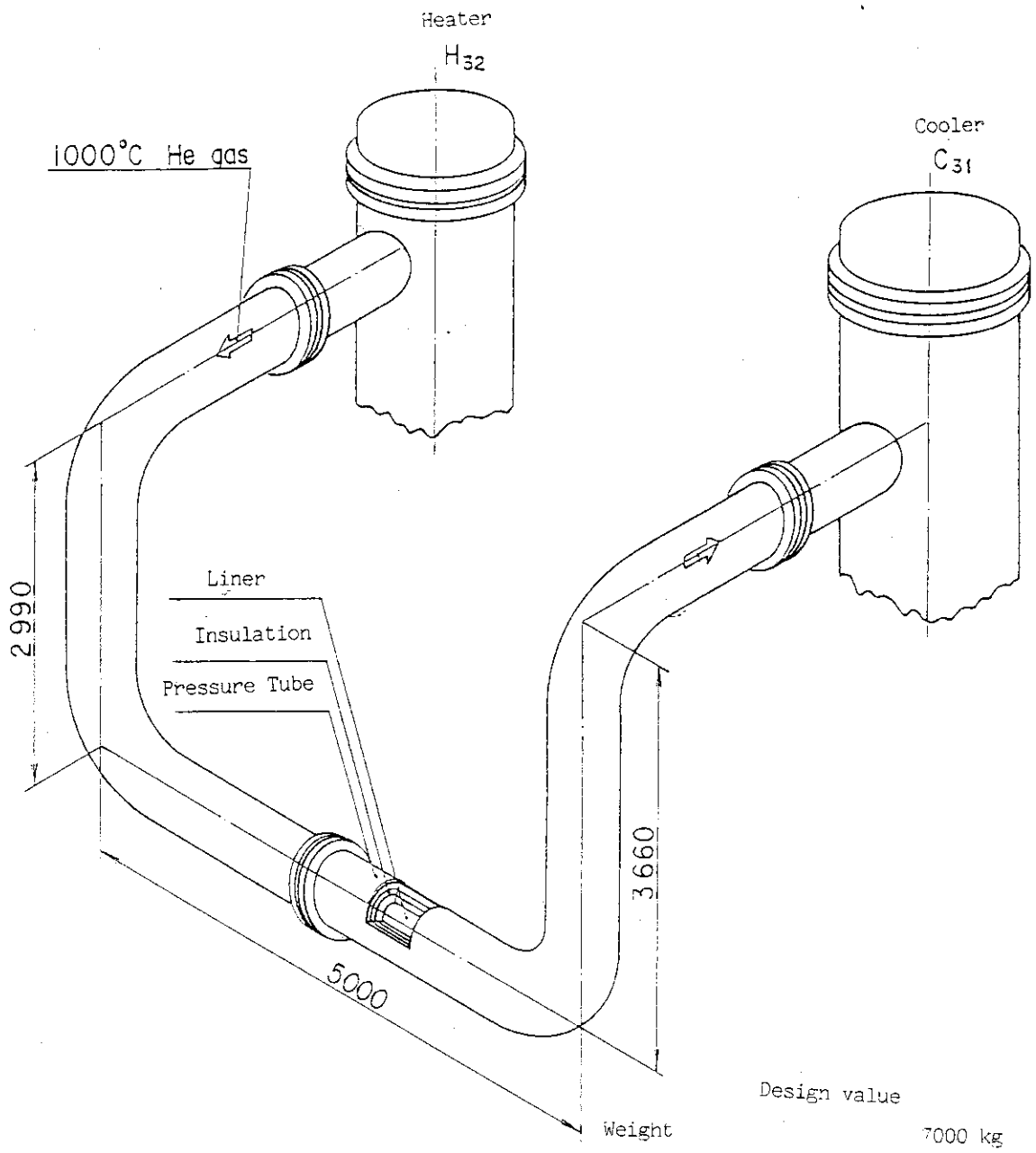

Design value	
Weight	7000 kg
Heat flux per unit length	7000 kcal/m
Flow rate	2.8 kg/s
Pressure	40 kg/cm^2g
Inlet temperature	1000 °C

Fig.3.1 Layout of the hot gas duct

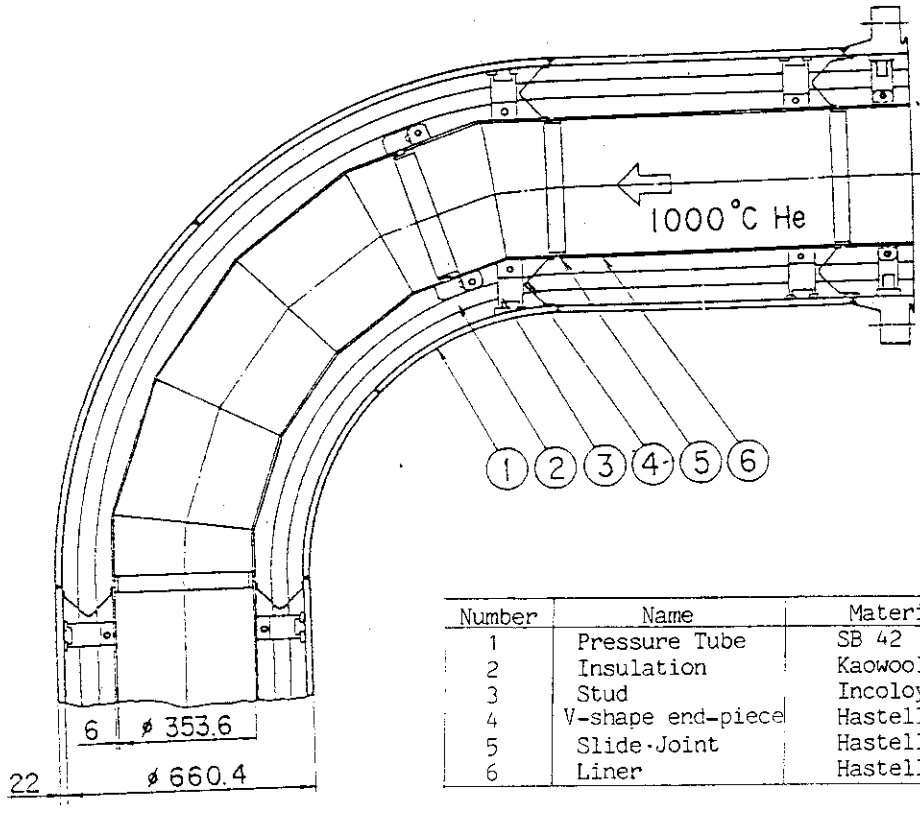

Number	Name	Material
1	Pressure Tube	SB 42
2	Insulation	Kaowool
3	Stud	Incoloy 800
4	V-shape end-piece	Hastelloy X
5	Slide·Joint	Hastelloy X
6	Liner	Hastelloy X

Fig.3.2 Cross section of the hot gas duct

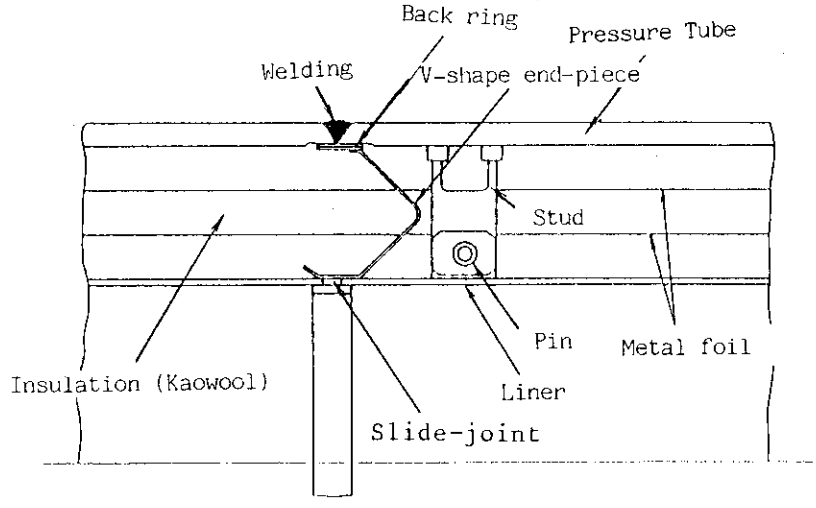

Fig.3.3 Detail of the hot gas duct

4. Temperature distribution measurement in the insulation layer

Temperature distribution within the insulation layer and along the V-shape end-piece were measured with thermocouples fixed at the cross section of horizontal hot gas ducts both at the outlet of the heater H32 and at the inlet of the cooler C31. The measuring points are shown in Fig. 4.1, and results during the test operation in Figs. 4.2∿4.13.

The maximum circumferential temperature difference of 100°C was observed, and this might be due to the nonuniformity of the insulation layer, or to the uncertainty of the locations of thermocouples.

Also those of the pressure tube were measured at the two cross sections in the middle part of the hot gas duct. The measuring points are shown in Fig. 4.1, measured data during the test operations in Figs. 4.14∿4.19. Temperature at the bottom is max. 30°C higher than at the top. This might be due to the cooling condition of ambient air.

Figures 4.20∿4.22 show the average radial temperature distribution within the insulation layer during the test operations, NO.1 and NO.2 cycle tests. Temperature distributions within the insulation layer were almost linear, and there was no significant indication of free convection occurring in the insulation.

Figures 4.23∿4.25 show temperatures in the insulation layer and V-shape end-piece at the outlet of the heater H32 versus helium gas temperature. Temperature gradient at each measuring points was almost uniform.

Measured data used in these figures are given in Appendix 1.

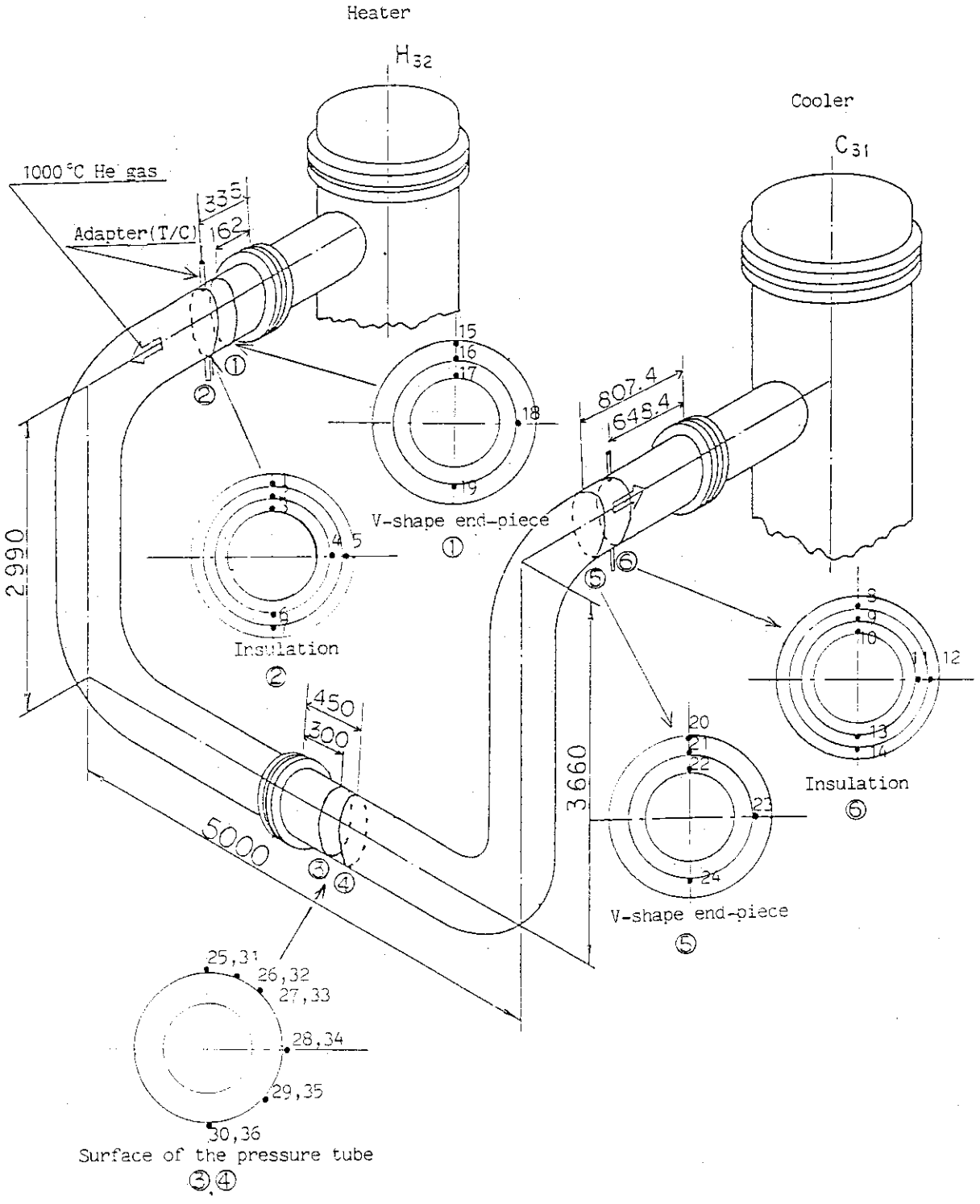

Fig. 4.1 Measuring points of the hot gas duct

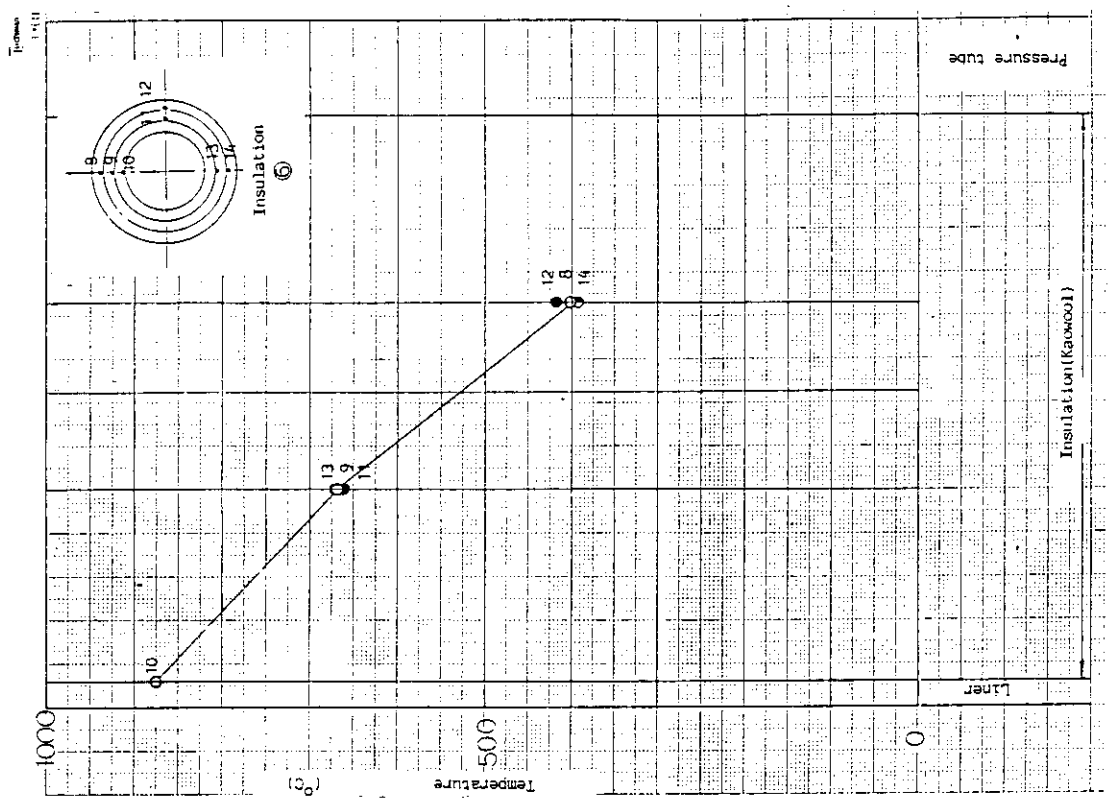

Fig. 4.3 Distribution of temperature in insulation at C_{31} side (flow rate 4.0 kg/s, He gas temperature 880°C).

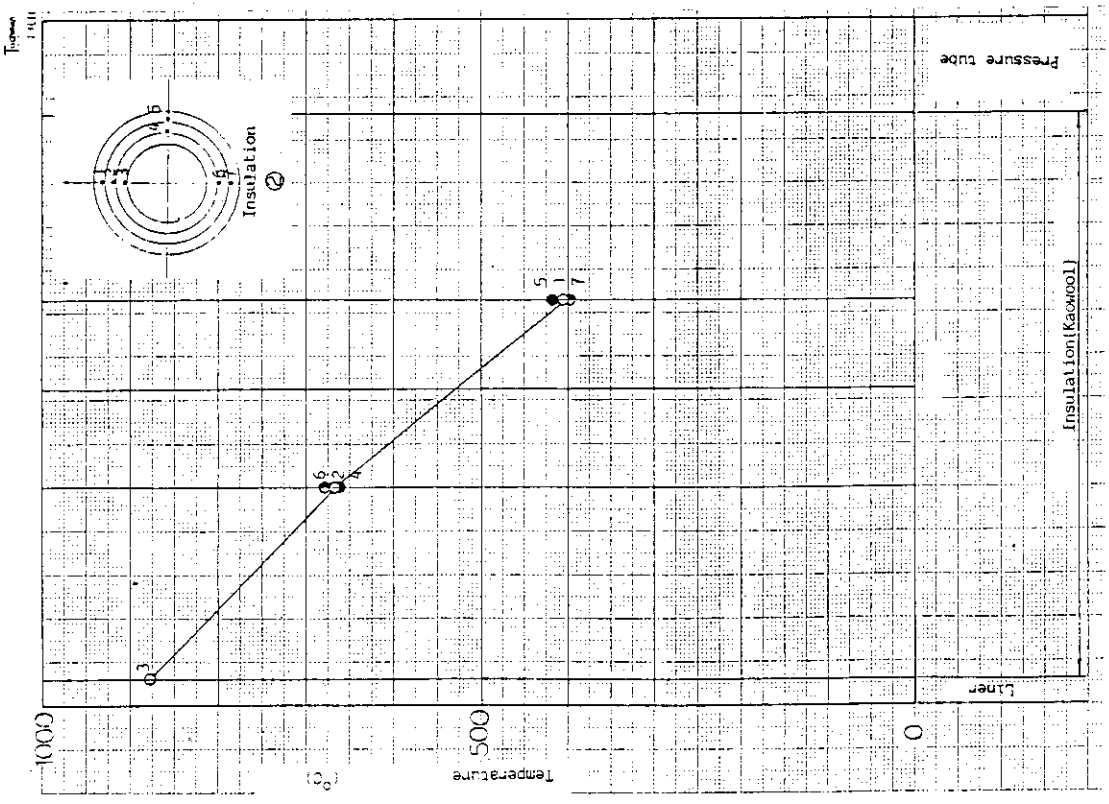

Fig. 4.2 Distribution of temperature in insulation at H_{32} side (flow rate 4.0 kg/s, He gas temperature 880°C).

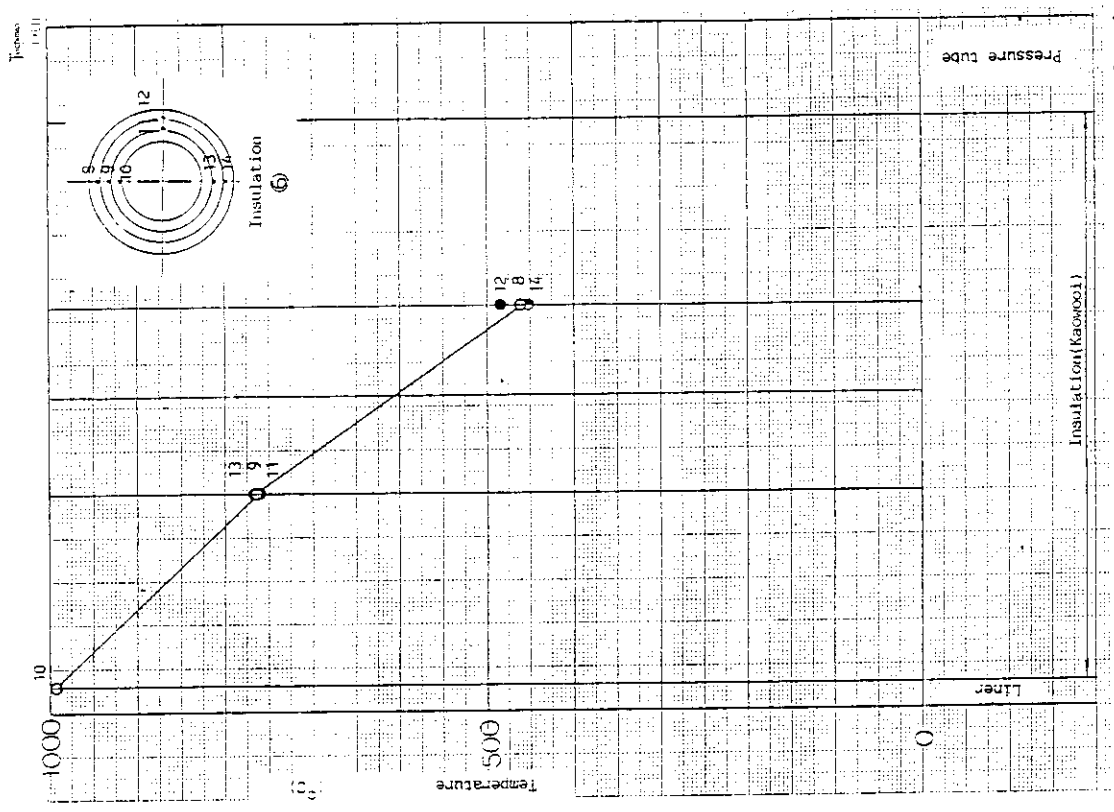

Fig. 4.5 Distribution of temperature in insulation at C_{31} side (flow rate 2.8 kg/s, He gas temperature 1000°C)

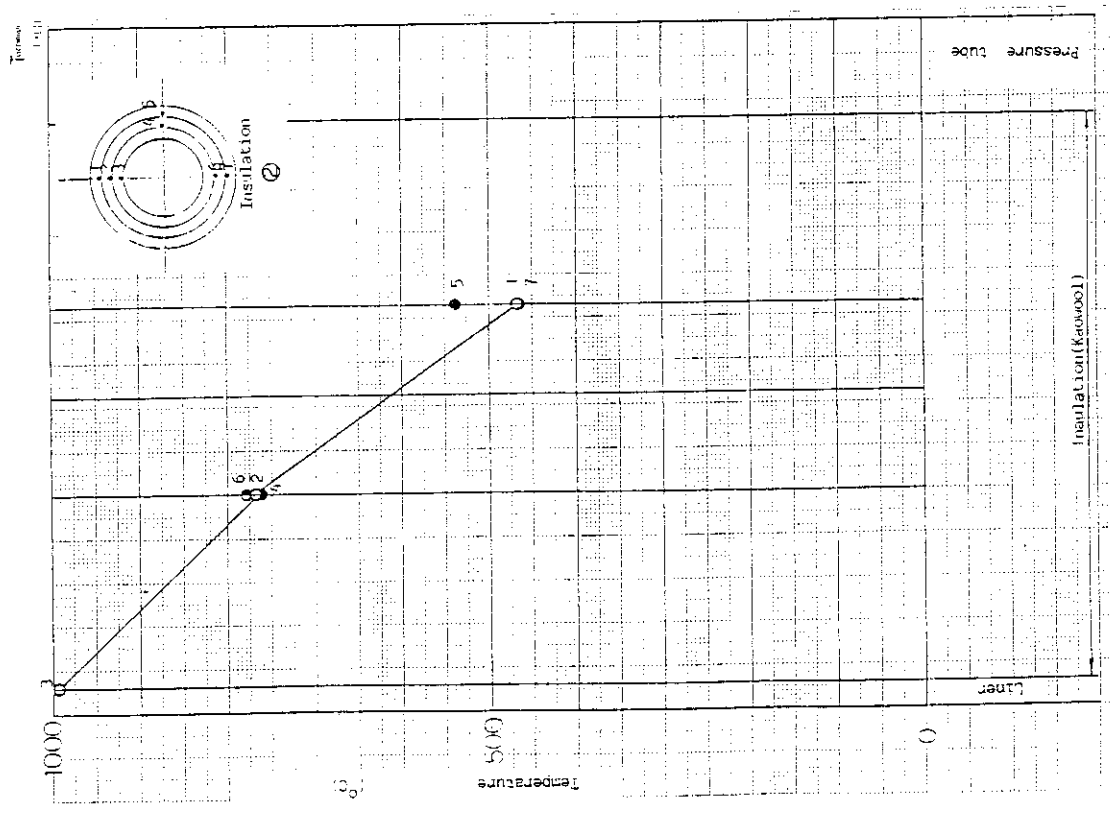

Fig. 4.4 Distribution of temperature in insulation at H_{32} side (flow rate 2.8 kg/s, He gas temperature 1000°C)

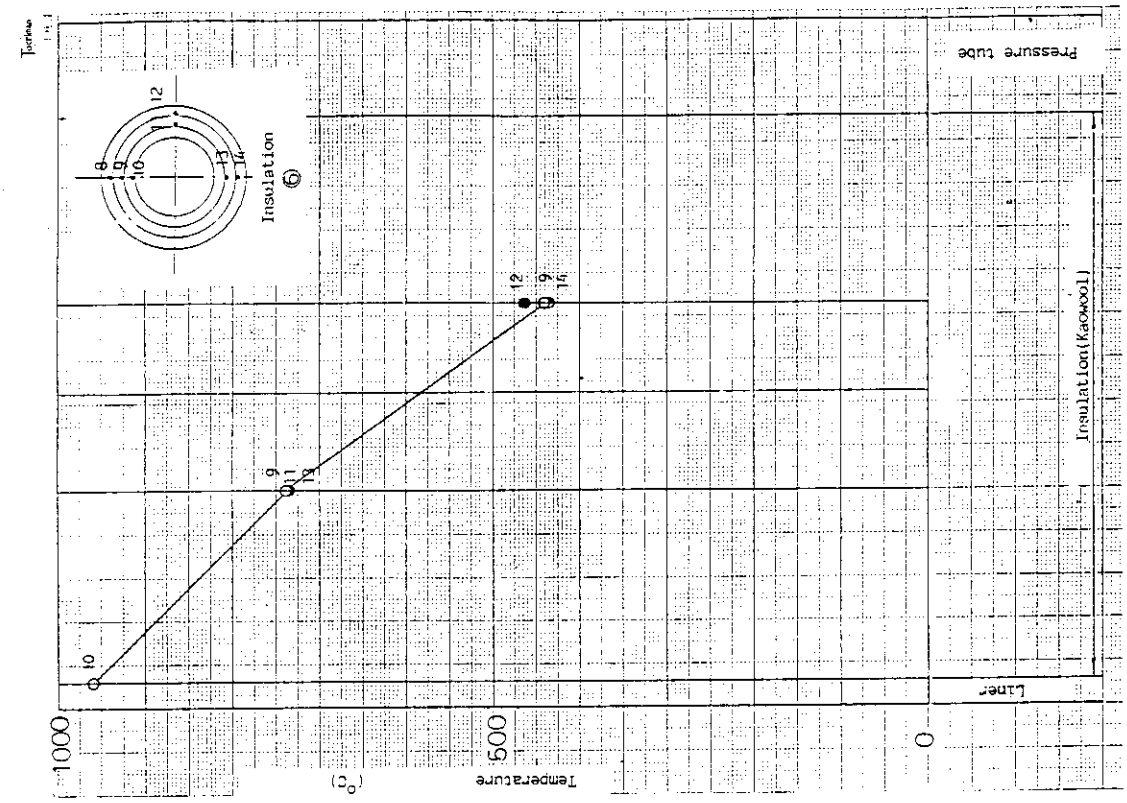

Fig. 4.7 Distribution of temperature in insulation at C_{31} side (flow rate 0.4 kg/s, He gas temperature 1000°C).

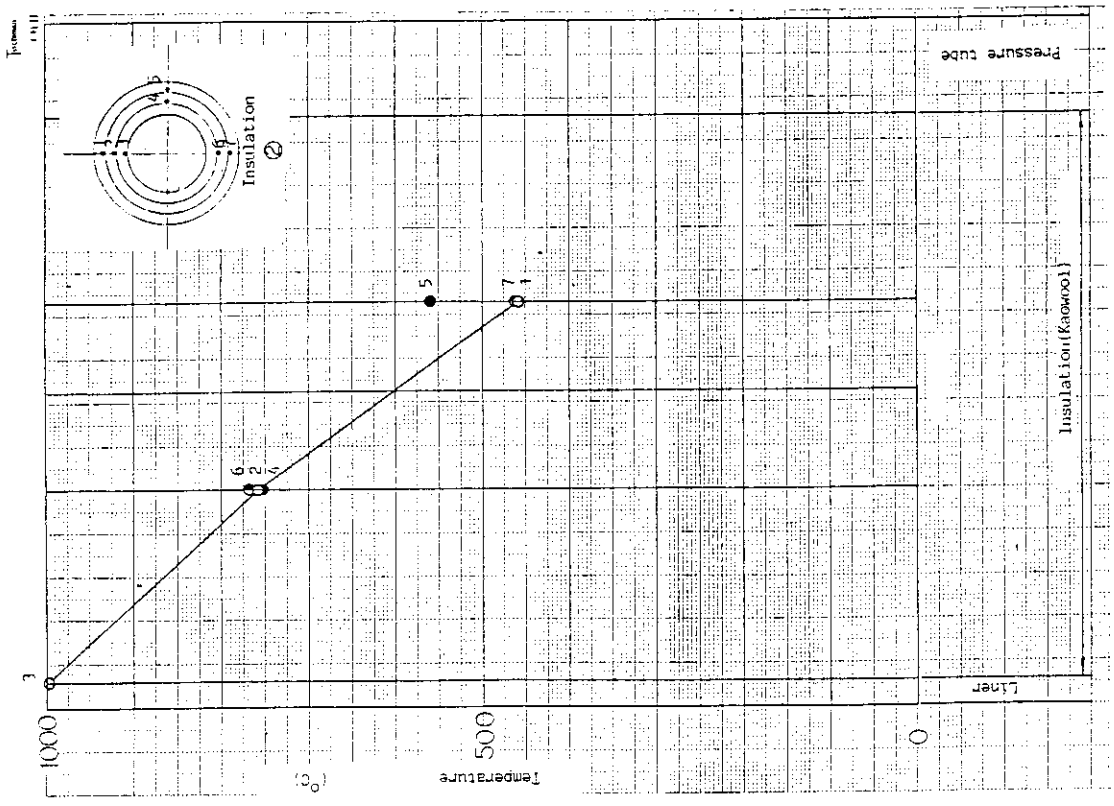

Fig. 4.6 Distribution of temperature in insulation at H_{32} side (flow rate 0.4 kg/s, He gas temperature 1000°C).

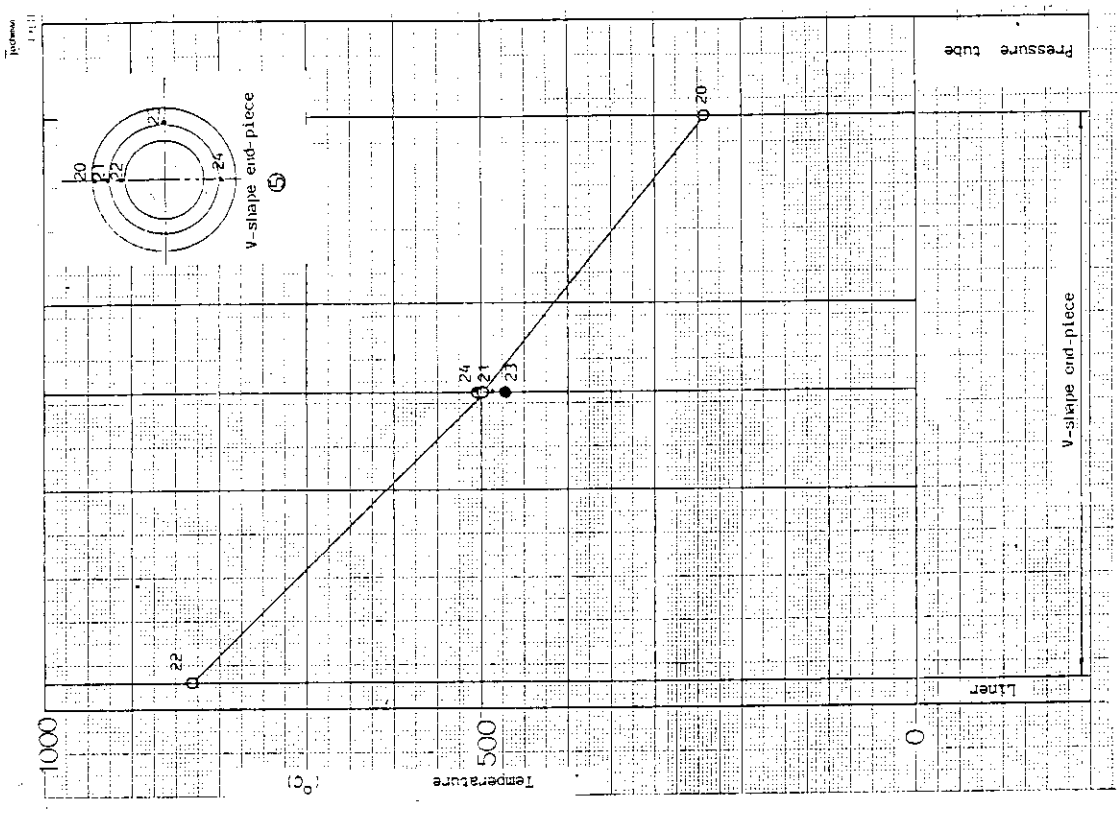

Fig. 4.9 Distribution of temperature in V-shape end-piece at C_{31} side (flow rate 4.0 kg/s, He gas temperature 880°C).

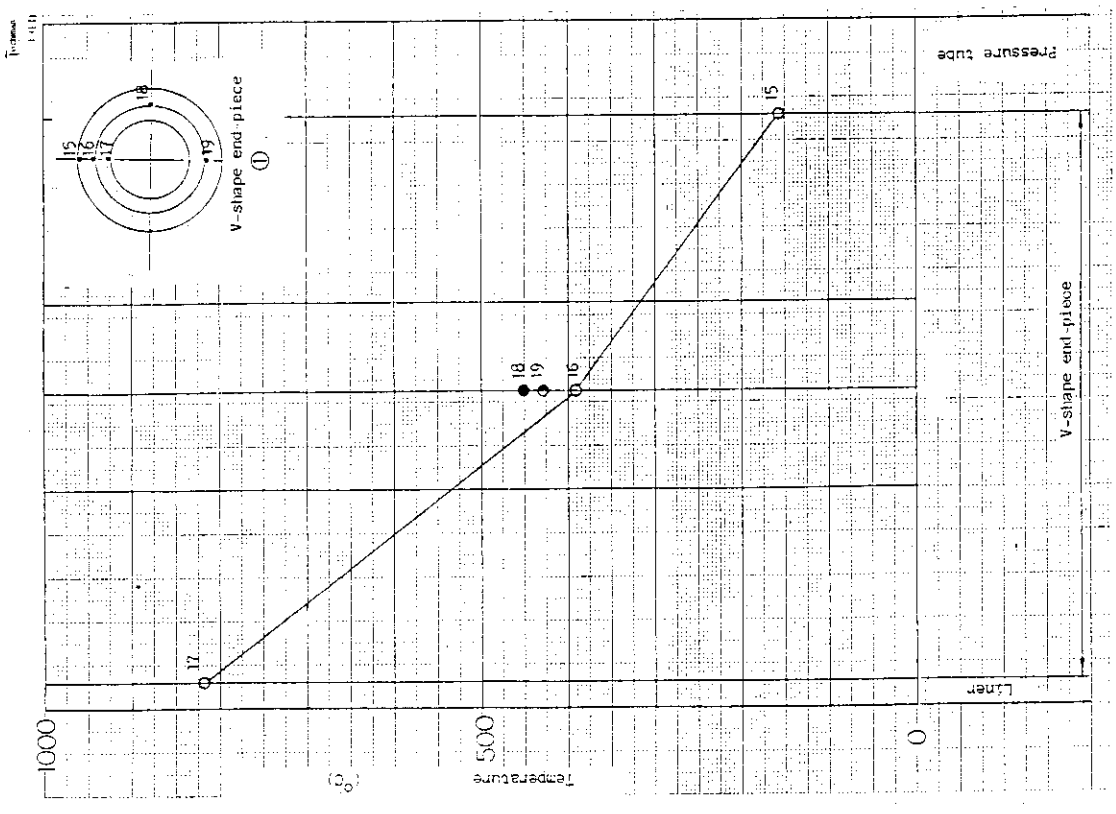

Fig. 4.8 Distribution of temperature in V-shape end-piece at H_{32} side (flow rate 4.0 kg/s, He gas temperature 880°C).

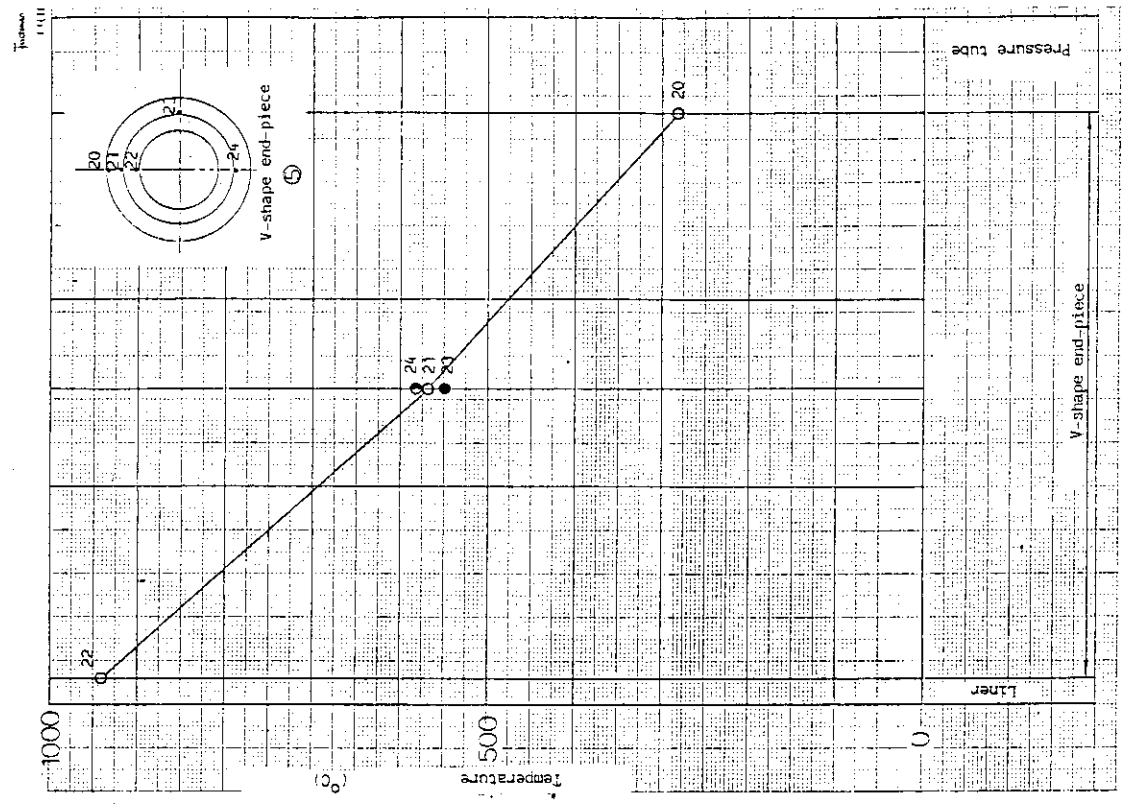

Fig. 4.11 Distribution of temperature in V-shape end-piece at C_{31} side (flow rate 2.8 kg/s, He gas temperature 1000°C).

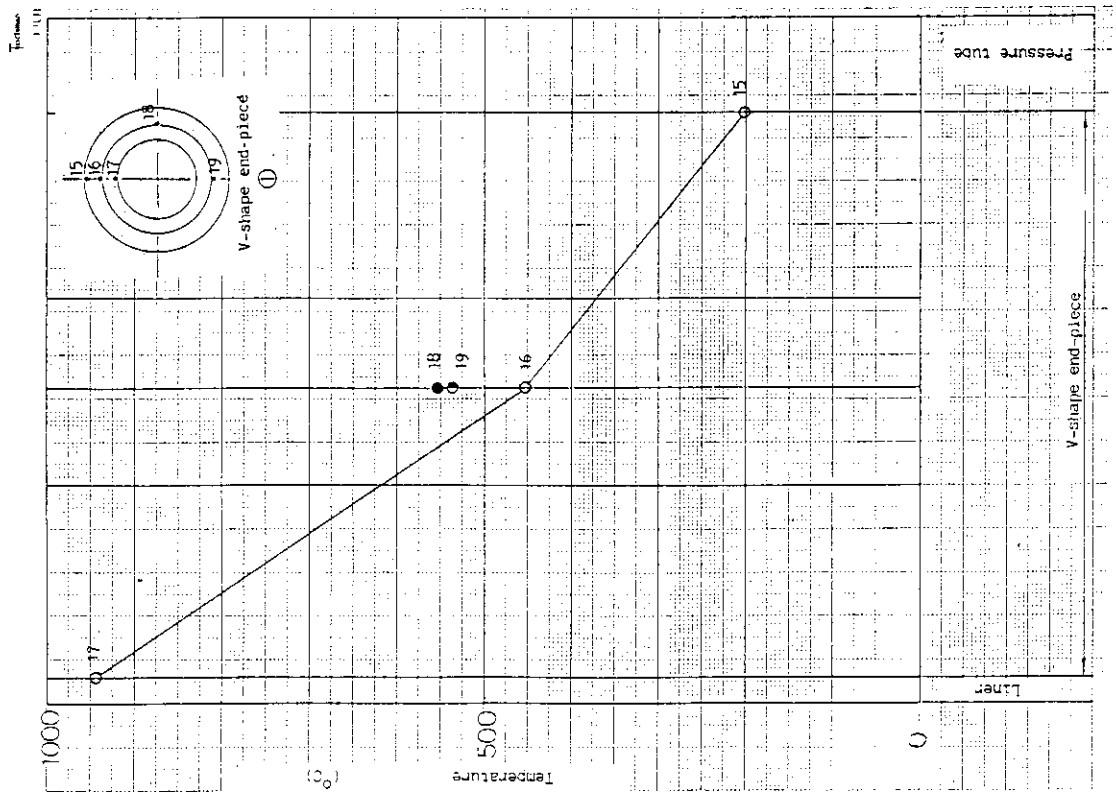

Fig. 4.10 Distribution of temperature in V-shape end-piece at H_{32} side (flow rate 2.8 kg/s, He gas temperature 1000°C).

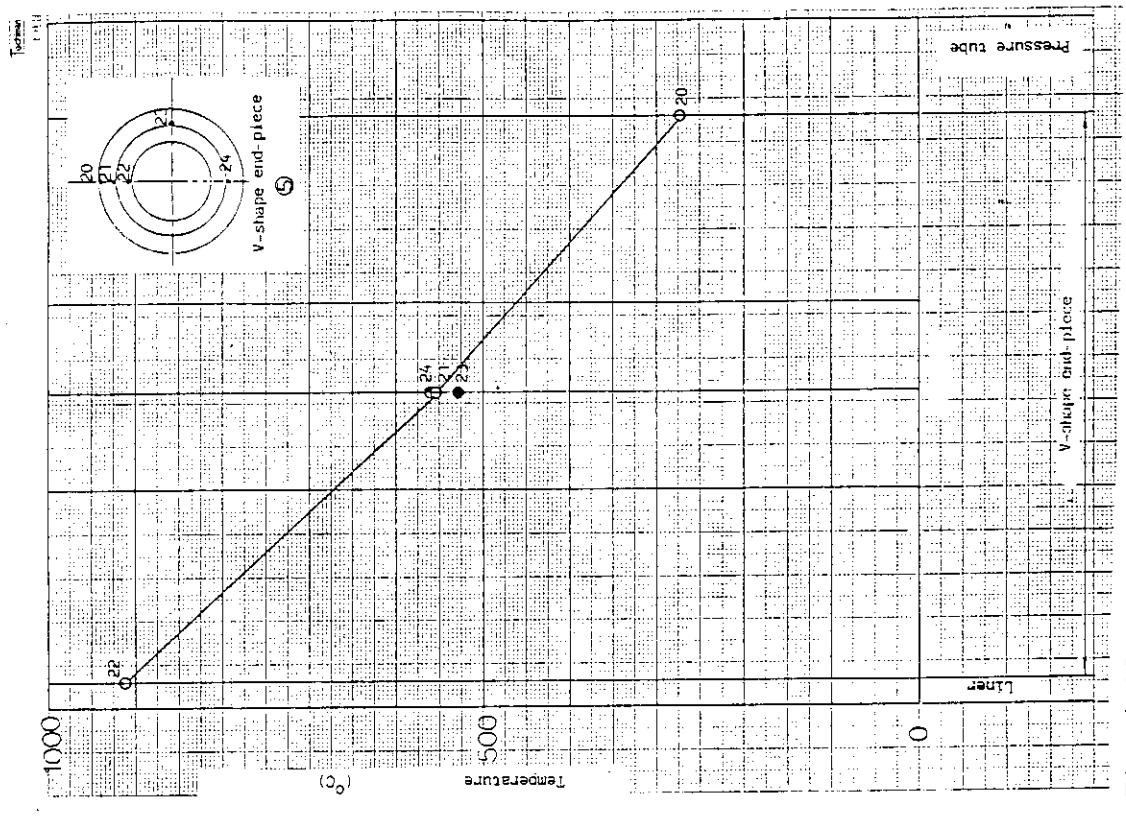

Fig. 4.13 Distribution of temperature in V-shape end-piece at C_{31} side (flow rate 0.4 kg/s, He gas temperature 1000°C).

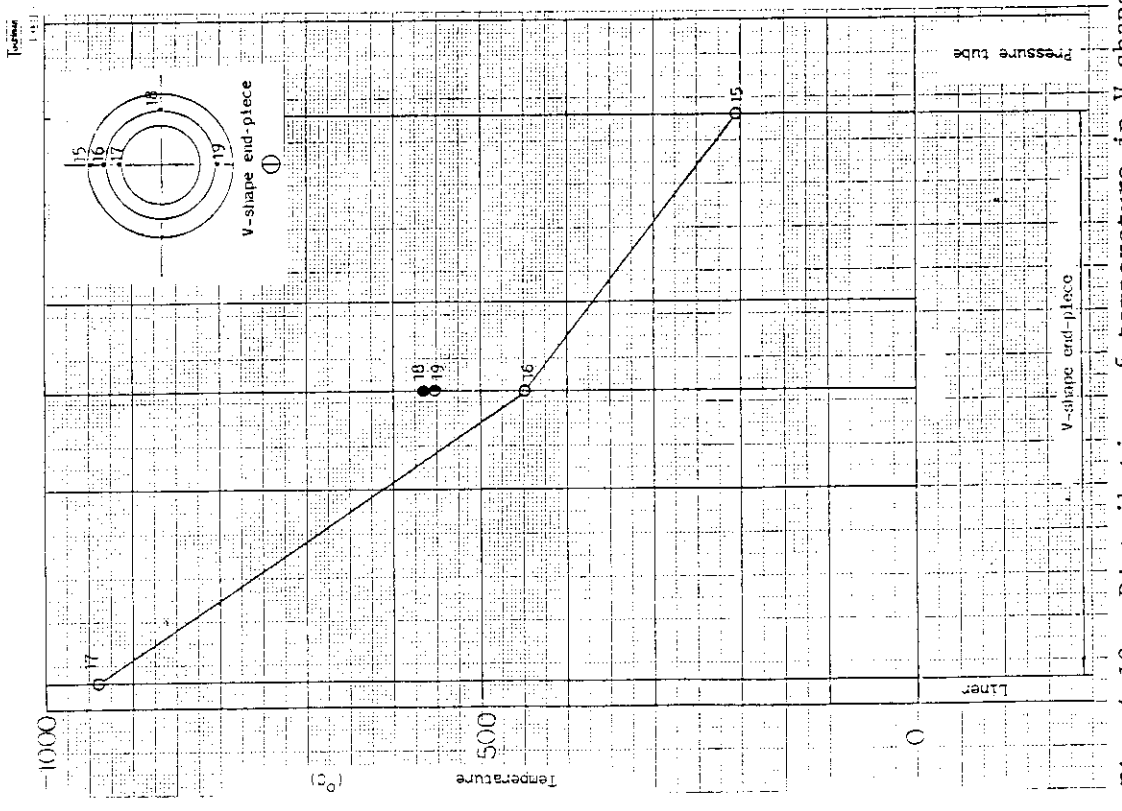

Fig. 4.12 Distribution of temperature in V-shape end-piece at H_{32} side (flow rate 0.4 kg/s, He gas temperature 1000°C).

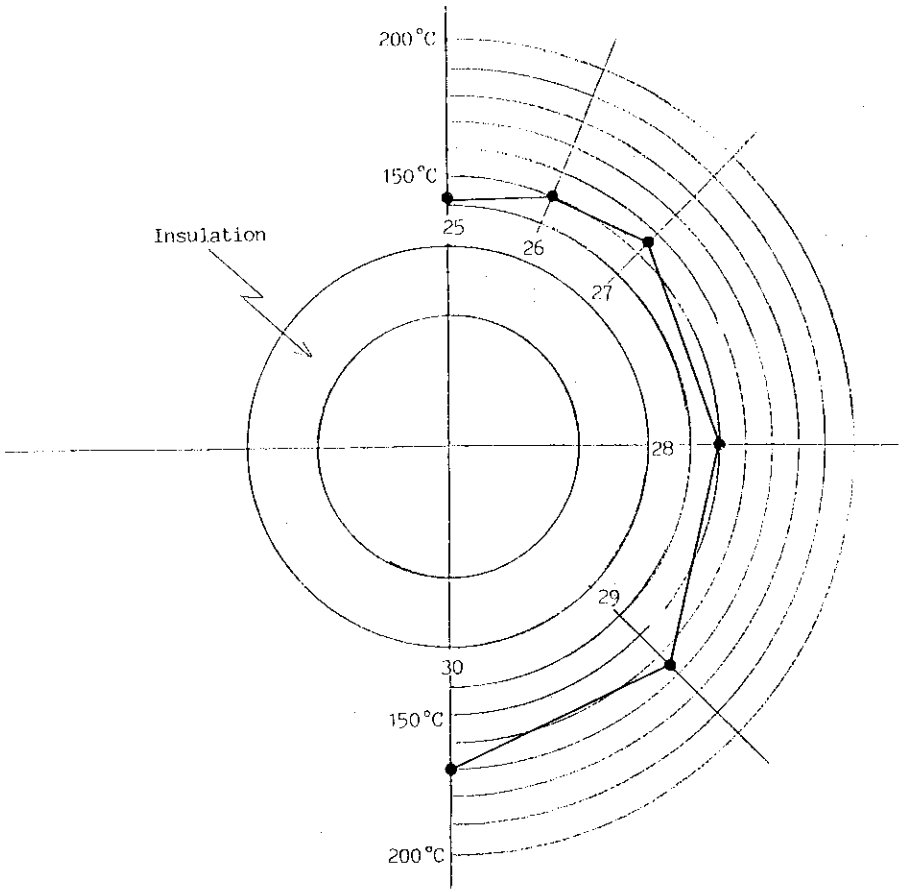

Fig. 4.14 Distribution of temperature at the surface of the pressure tube (flow rate 4.0 kg/s, He gas temperature 880°C).

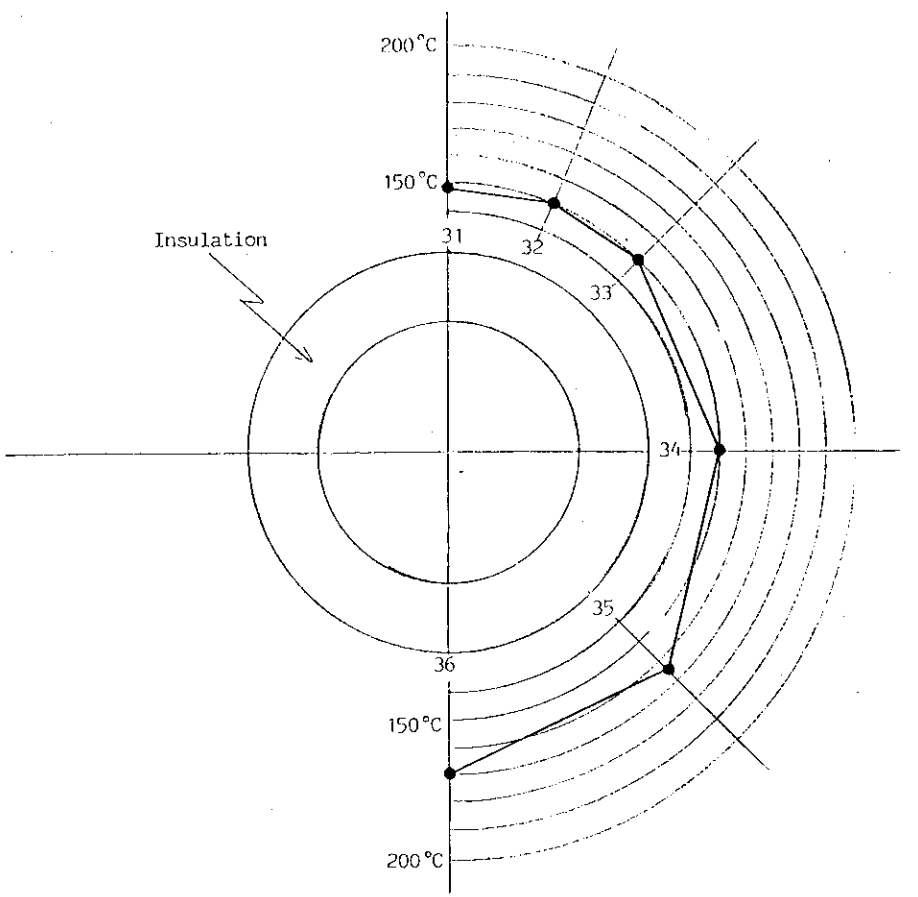

Fig. 4.15 Distribution of temperature at the surface of the pressure tube (flow rate 4.0 kg/s, He gas temperature 880°C).

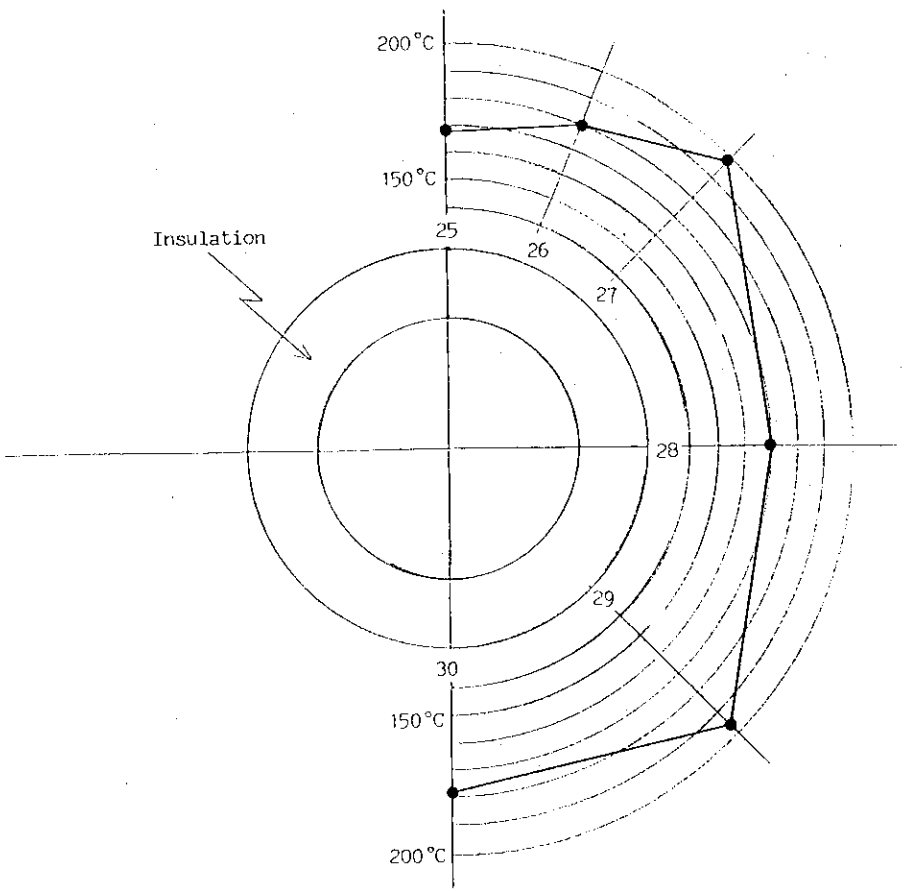

Fig. 4.16 Distribution of temperature at the surface of the pressure tube (flow rate 2.8 kg/s, He gas temperature 1000°C).

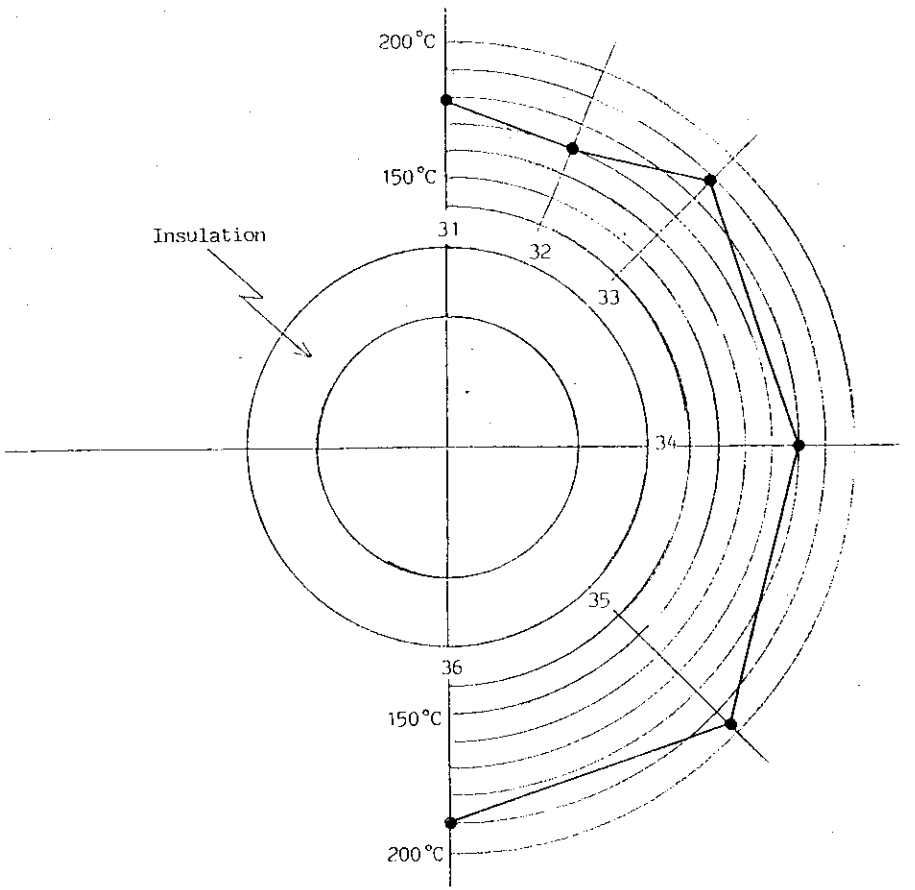

Fig. 4.17 Distribution of temperature at the surface of the pressure tube (flow rate 2.8 kg/s, He gas temperature 1000°C).

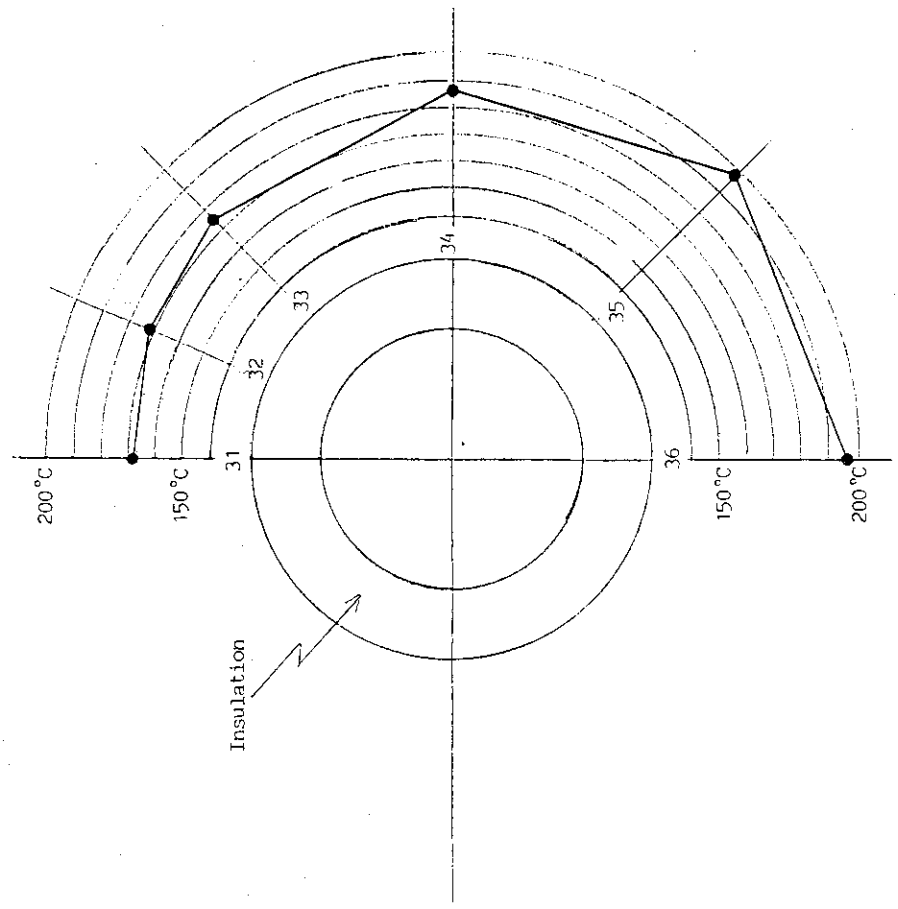

Fig. 4.19 Distribution of temperature at the surface of the pressure tube (flow rate 0.4 kg/s, He gas temperature 1000°C).

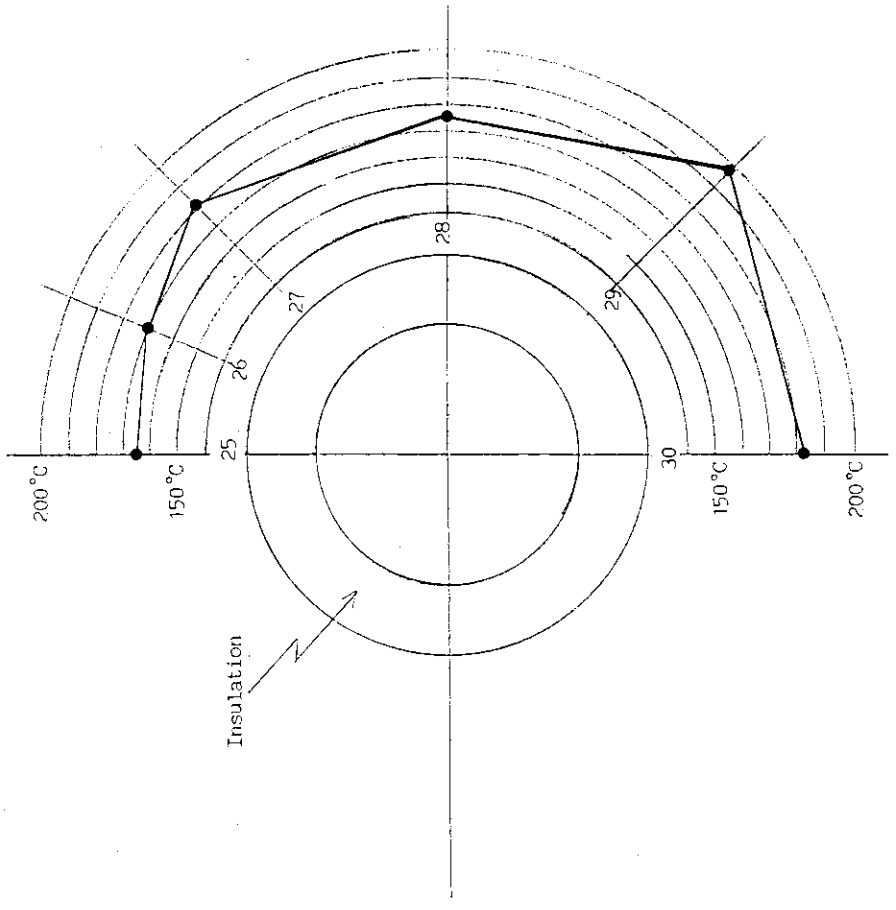

Fig. 4.18 Distribution of temperature at the surface of the pressure tube (flow rate 0.4 kg/s, He gas temperature 1000°C).

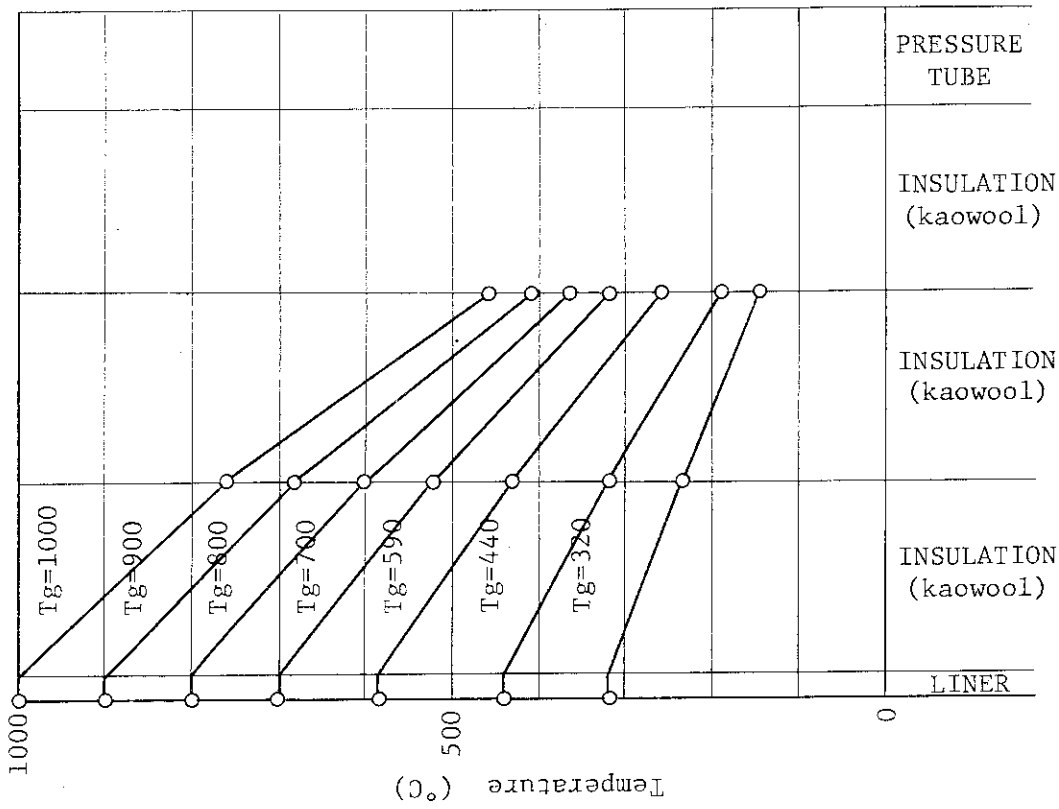

Fig. 4.21 Average radial temperature distribution of the hot gas duct (No.1 cycle test)
Tg : Helium gas temperature

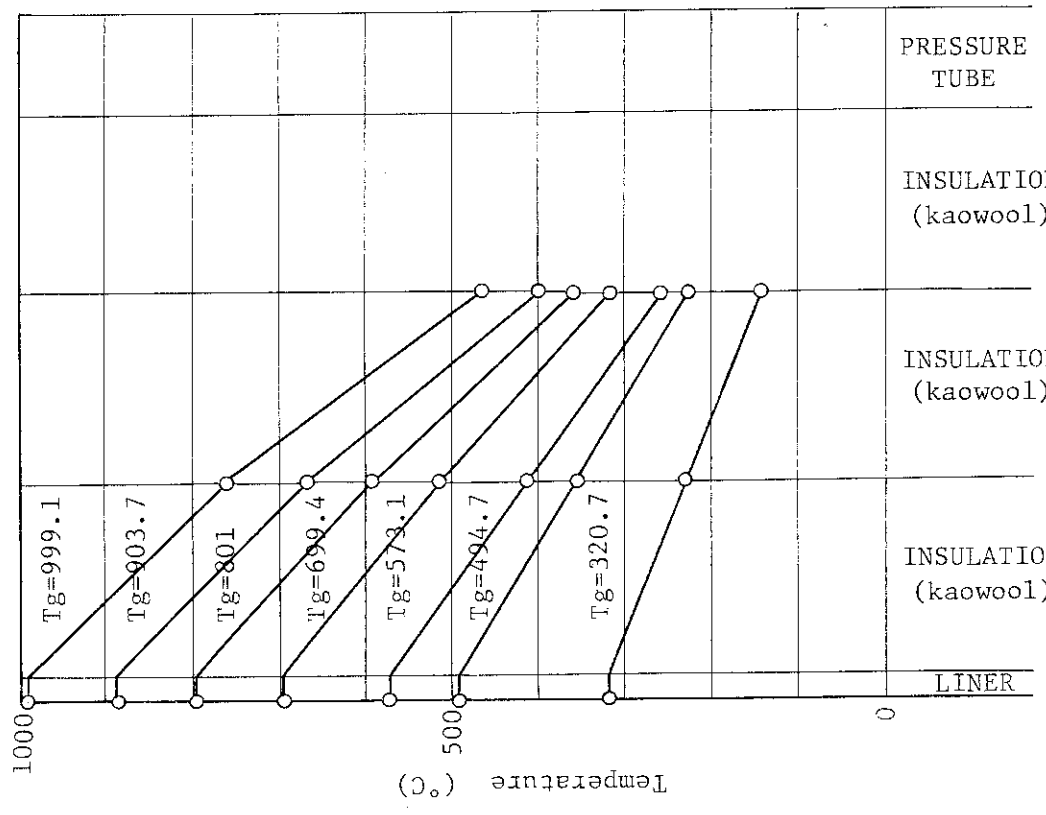

Fig. 4.20 Average radial temperature distribution of the hot gas duct (test operation)

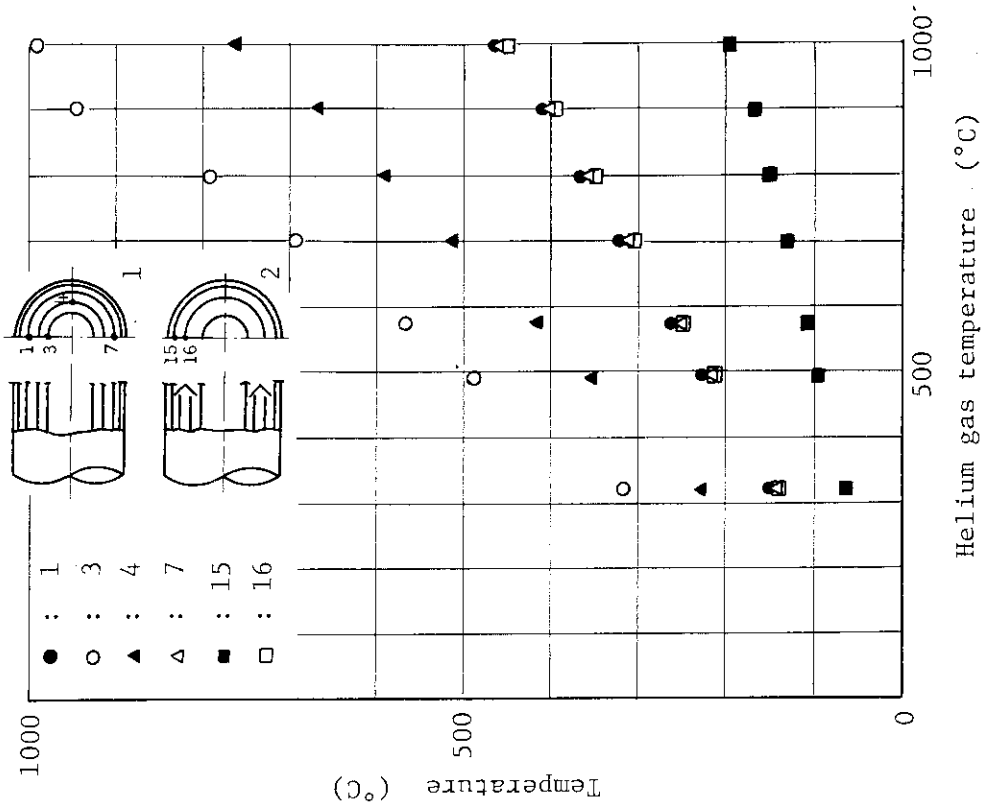

Fig. 4.23 Temperature within the insulation and V-shape end-piece (test operation)
Tg : Helium gas temperature

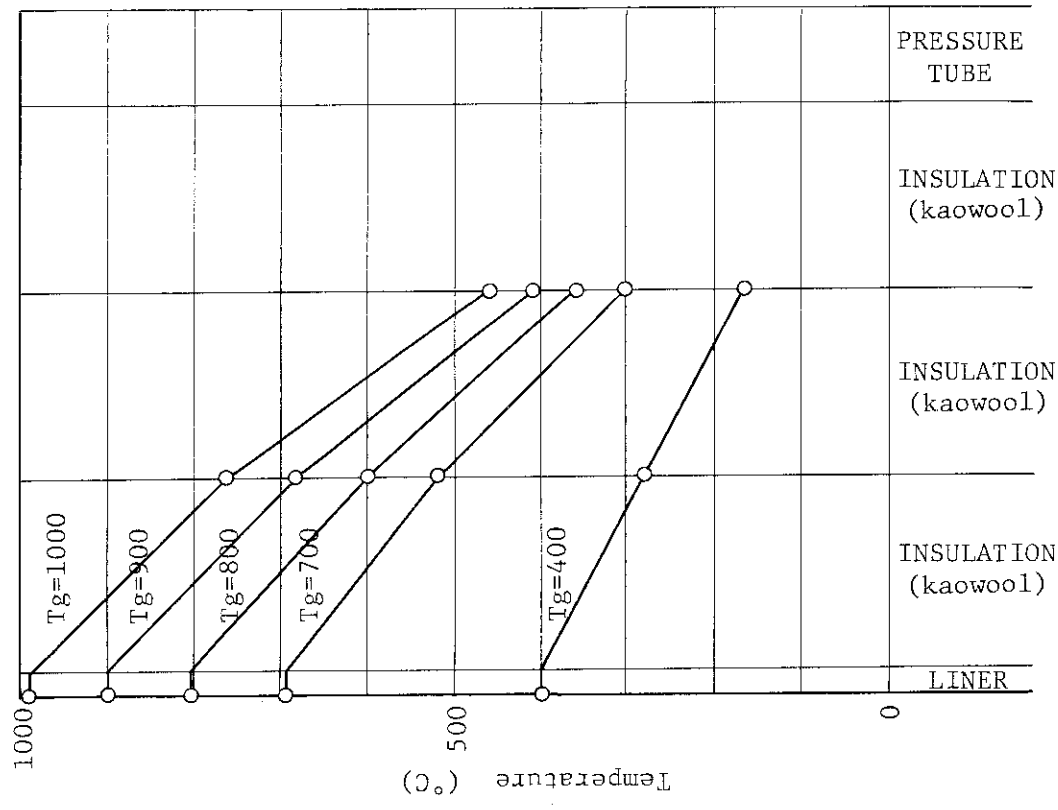

Fig. 4.22 Average radial temperature distribution of the hot gas duct (No.2 cycle test)

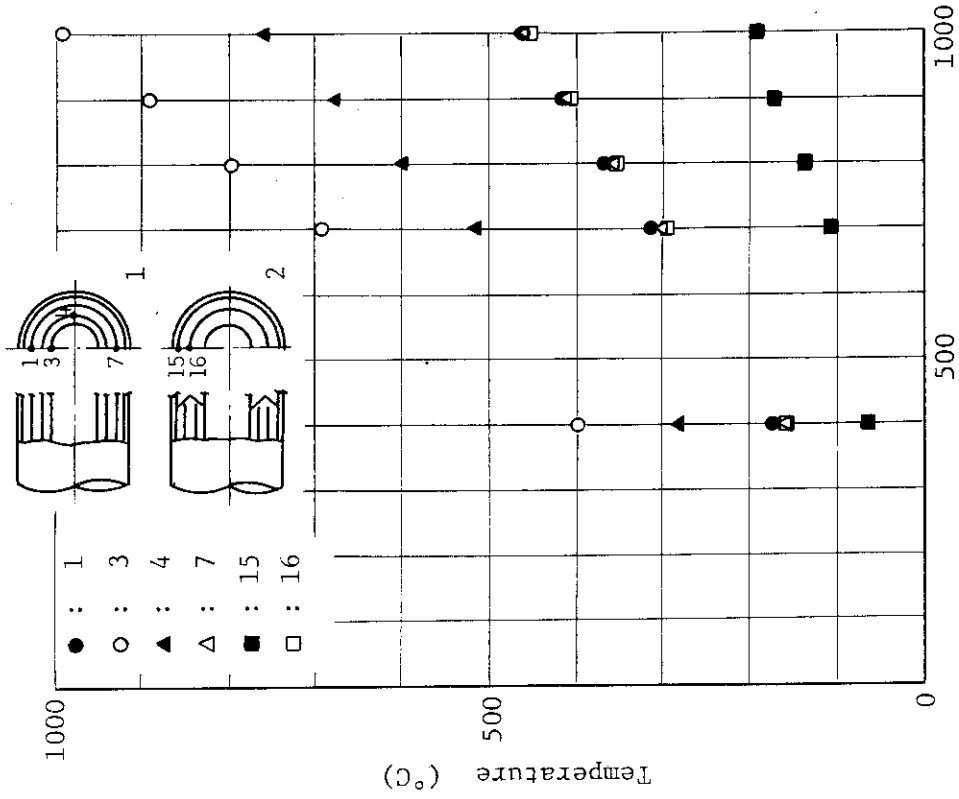

Fig. 4.25 Temperature within the insulation and V-shape end-piece (No.2 cycle test)

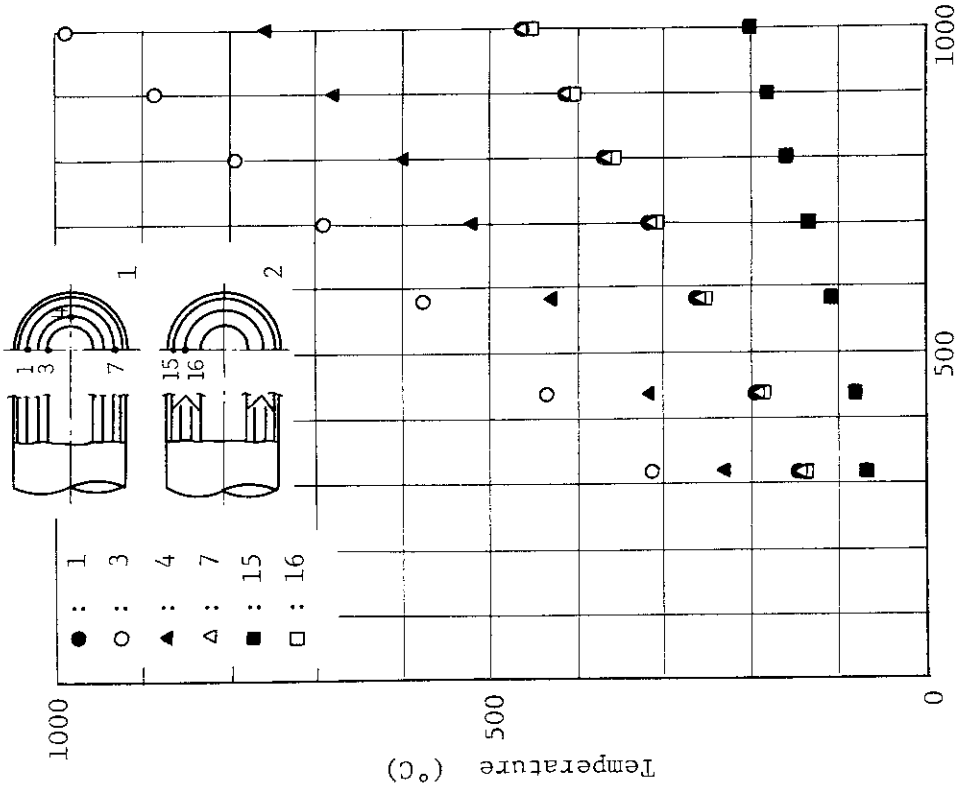

Fig. 4.24 Temperature within the insulation and V-shape end-piece (No.1 cycle test)

5. Effective thermal conductivity of the insulation layer

Figure 5.1 shows the dependence of the effective thermal conductivity upon the average temperatures of the insulation.

Under the assumption: the heat transfer coefficient at the outer surface of the pressure tube is about 12 kcal/m^{2}h°C, the heat transfer through insulation includes radiation (thermal emissivity is assumed to be 0.5), and the room temperature is 20 °C; the effective thermal conductivity of the insulation was calculated to be 0.4∿0.49 kcal/mh°C (0.47∿0.56 W/m°C) at the average temperature of the insulation during the three operations, namely 590 °C. The results are in approximate agreement with the data obtained by IHI Co., Ltd.

The calculating method of the effective thermal conductivity is described in Appendix 2.

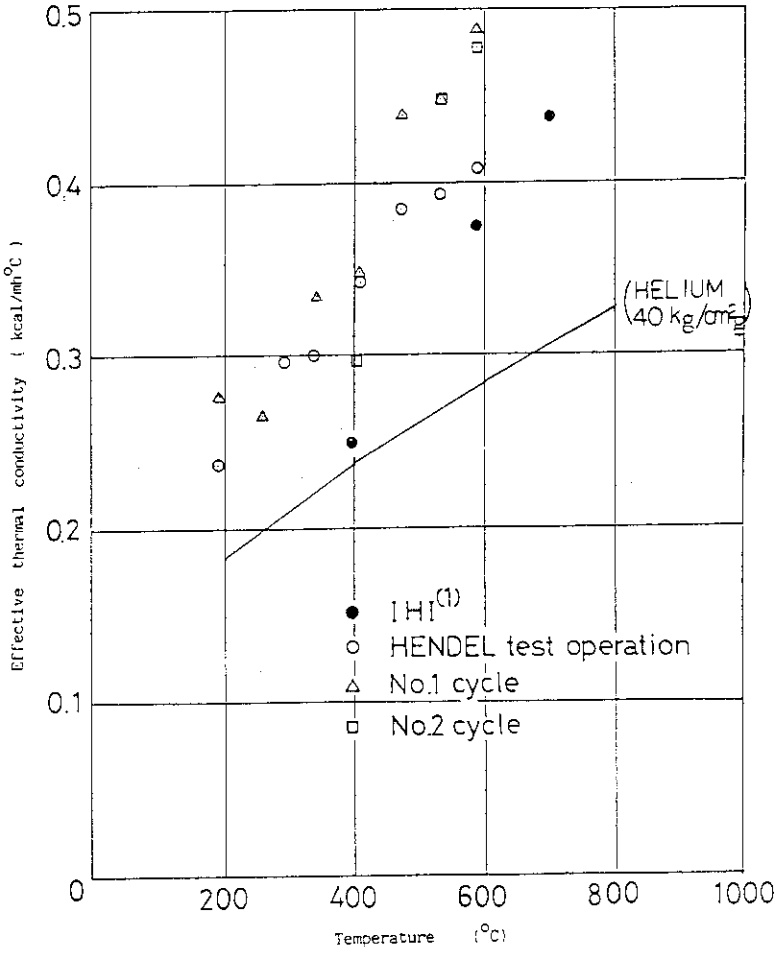

Fig. 5.1 Effective thermal conductivity of the hot gas duct.

6. Temperature distribution measurements of the pressure tube

(1) Measurement with a contacting thermometer

This has been performed to check the local temperature rise (hot spot) or degradations due to malfunction of the insulation layer. There was no hot spot as the surface of the pressure tubes with studs and V-shape end-pieces. The temperature at the top of the hot gas duct was not always higher than at the bottom. This is seemingly due to nonuniform convection of air around the hot gas duct.

The measured data shown in Figs. 6.1∿6.17 were taken during NO.1 cycle test.

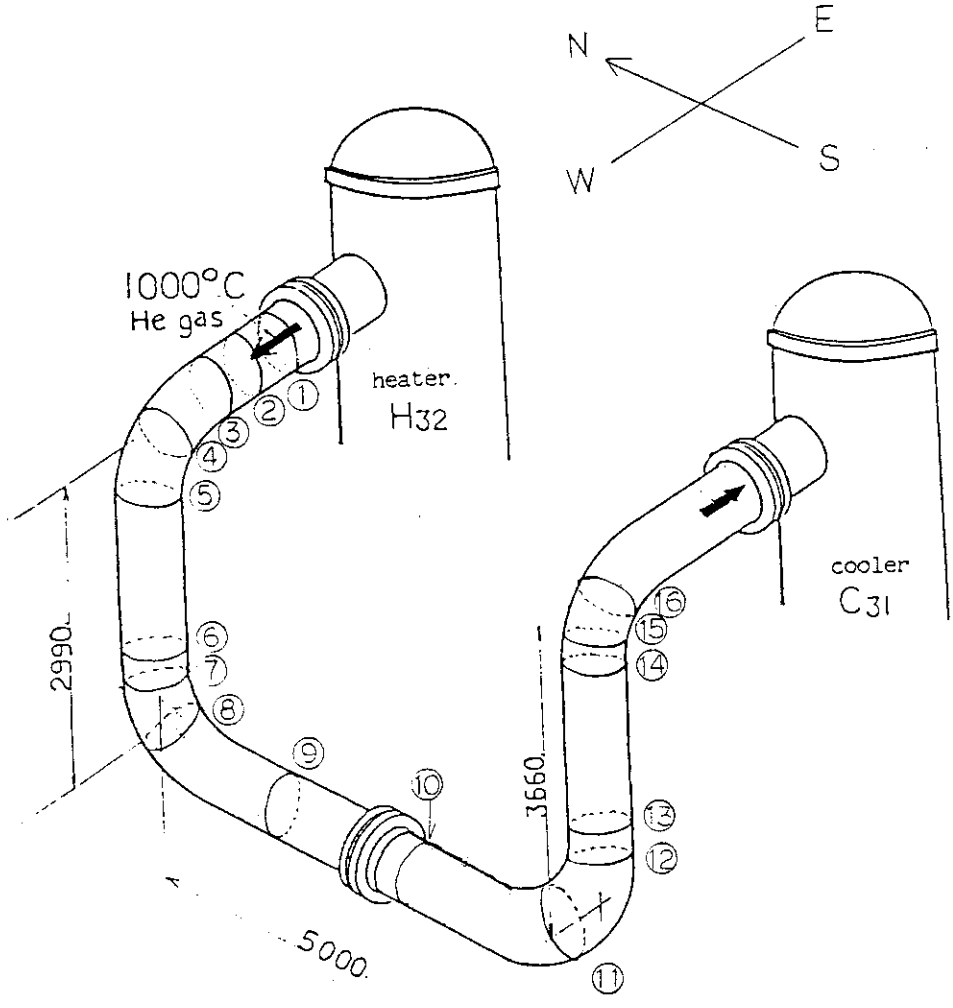

Fig.6.1 Measuring points at the surface of the hot gas duct

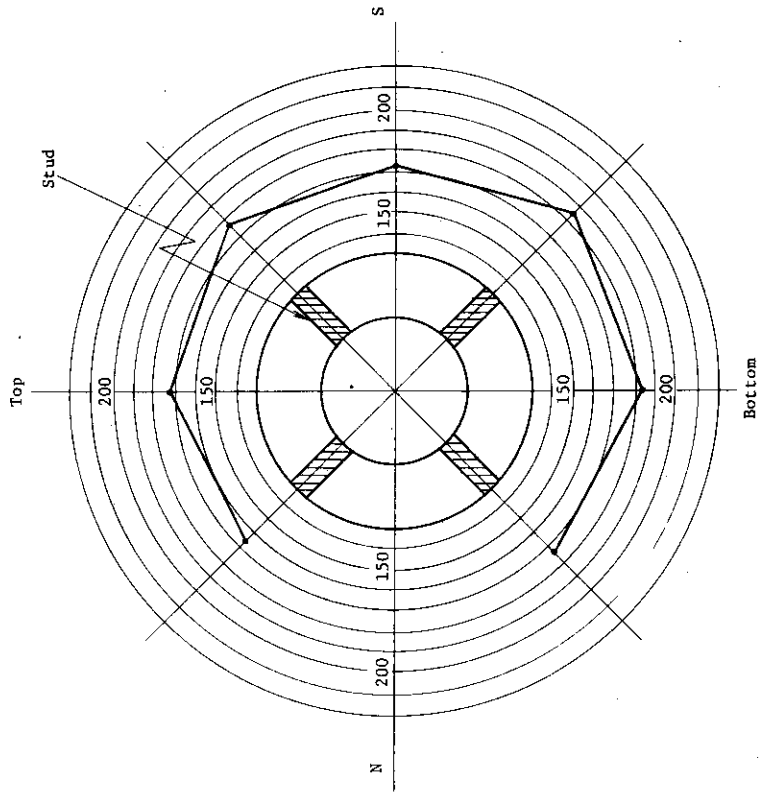

Fig. 6.3 Stud at H32 side

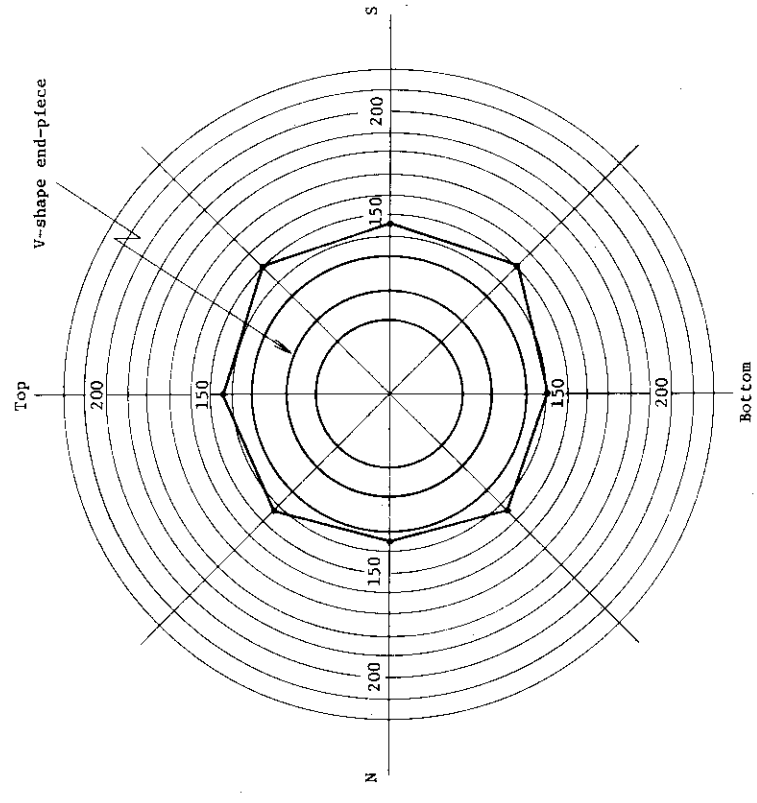

Fig. 6.2 V-shape end-piece at H32 side

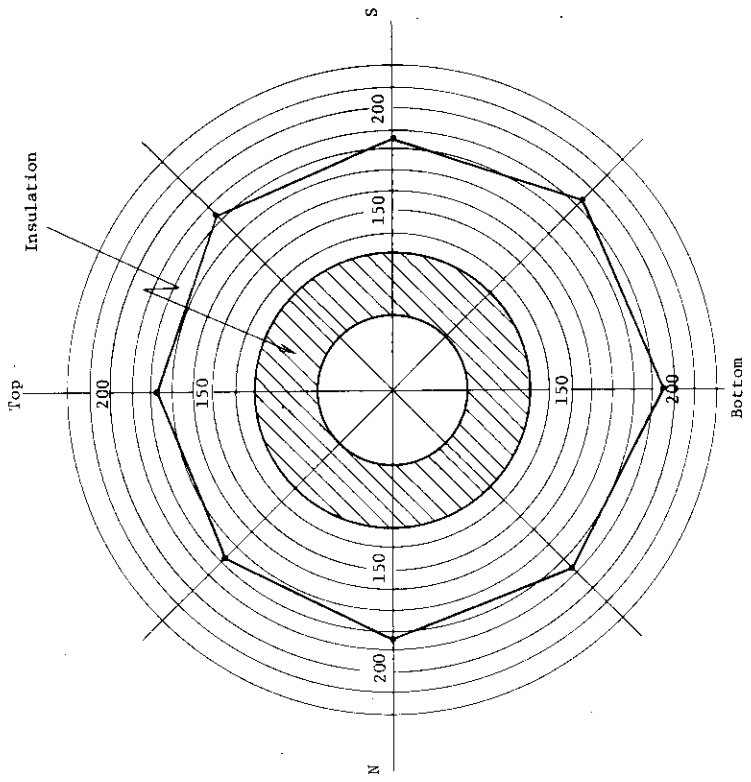

Fig. 6.5 First elbow of the hot gas duct

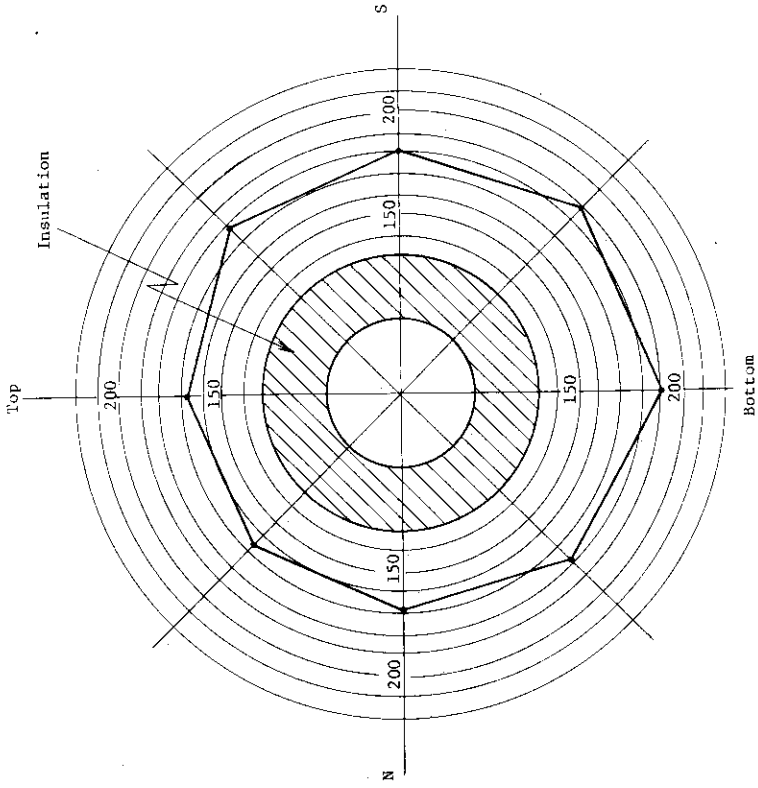

Fig. 6.4 Horizontal part of the hot gas duct at H32 side

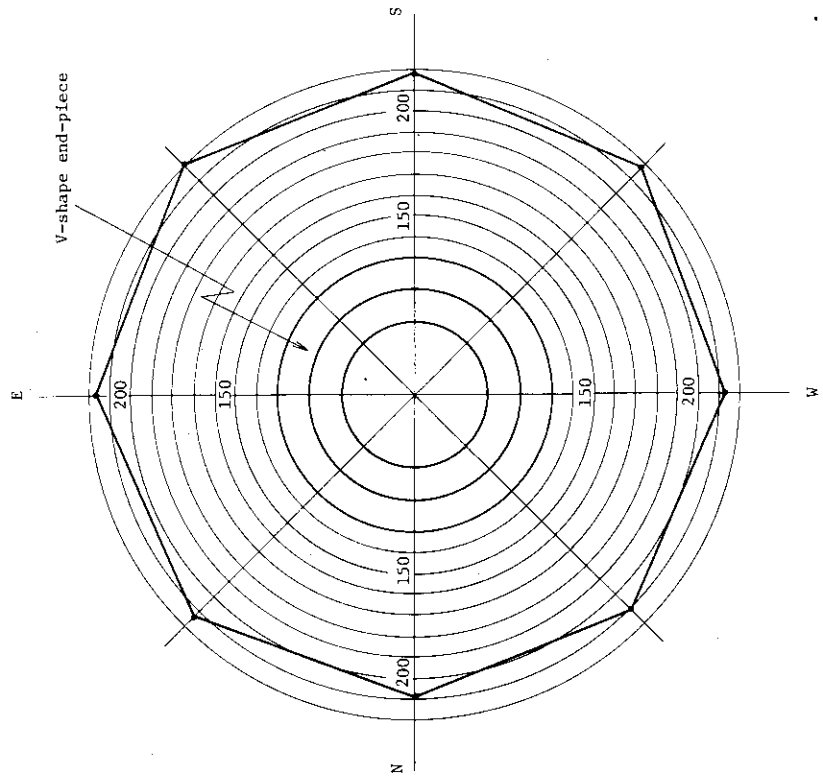

Fig. 6.7 V-shape end-piece of lower and perpendicular part of the hot gas duct at H32 side

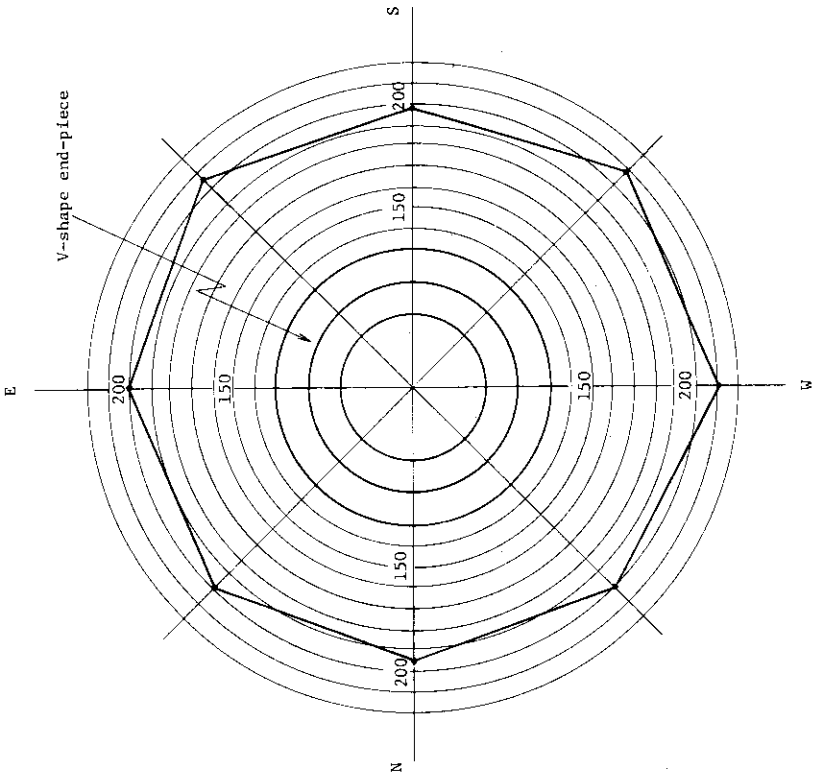

Fig. 6.6 V-shape end-piece of upper and perpendicular part of the hot gas duct at H32 side

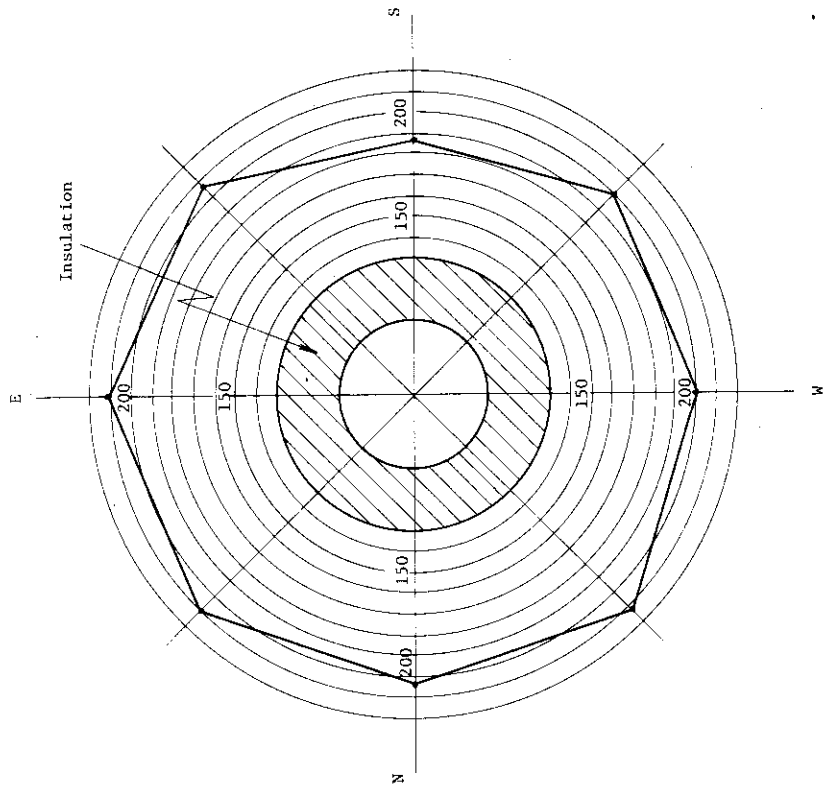

Fig. 6.9 Second elbow of the hot gas duct

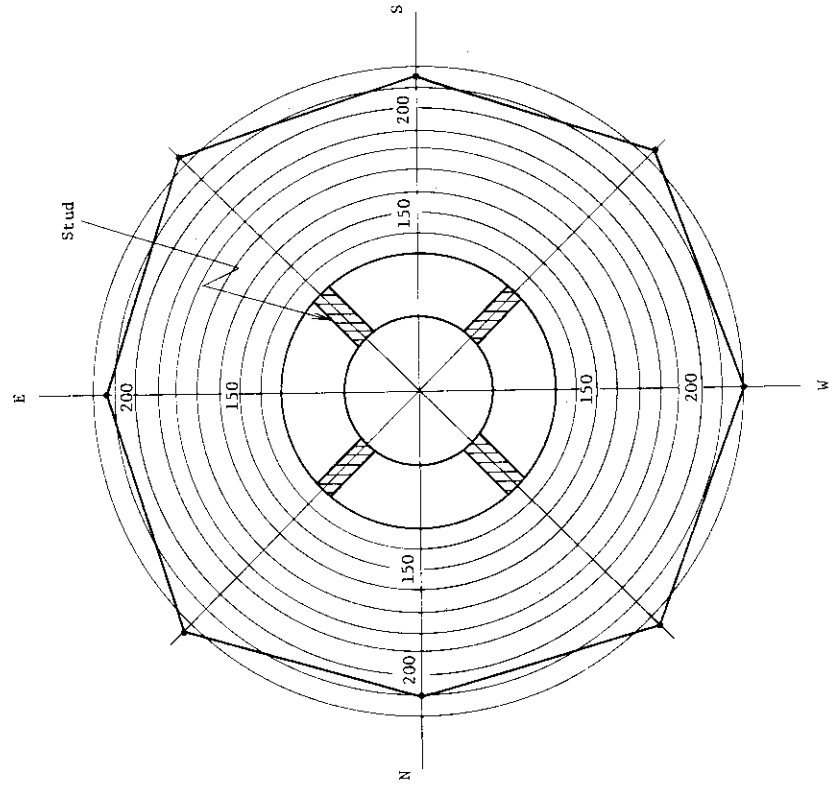

Fig. 6.8 Stud of lower and perpendicular part of the hot gas duct at H32 side

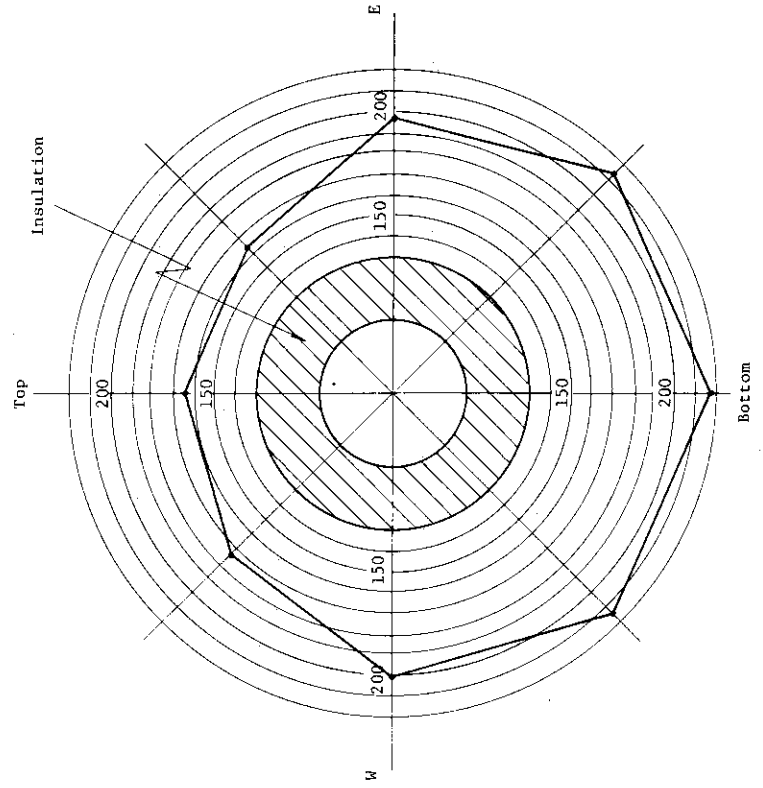

Fig. 6.11 Lower and horizontal part of the hot gas duct at H32 side

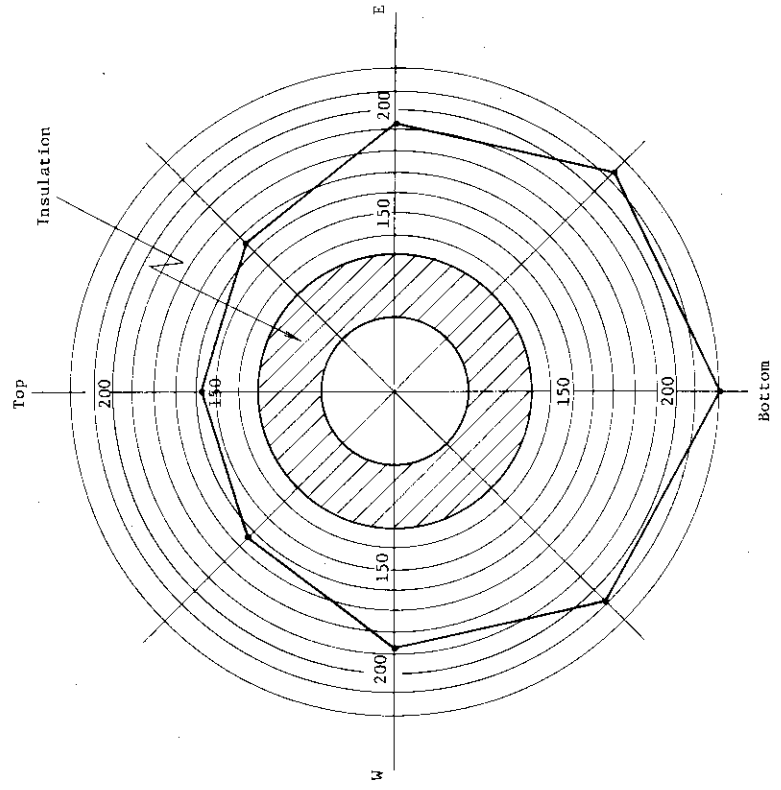

Fig. 6.10 Lower and horizontal part of the hot gas duct at H32 side

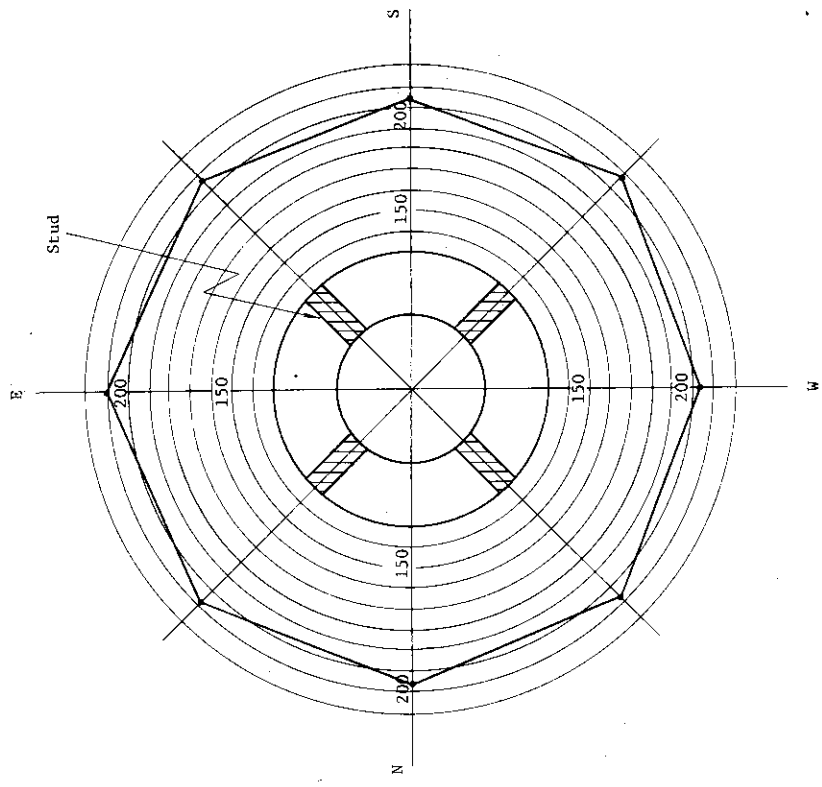

Fig. 6.13 Stud of lower and perpendicular part of the hot gas duct at C31 side

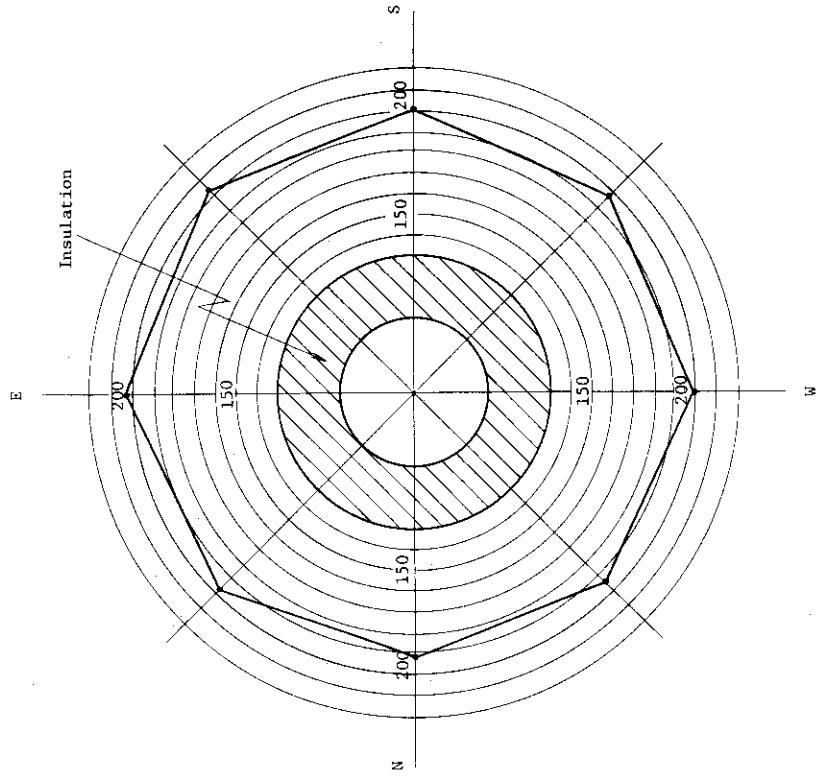

Fig. 6.12 Third elbow of the hot gas duct

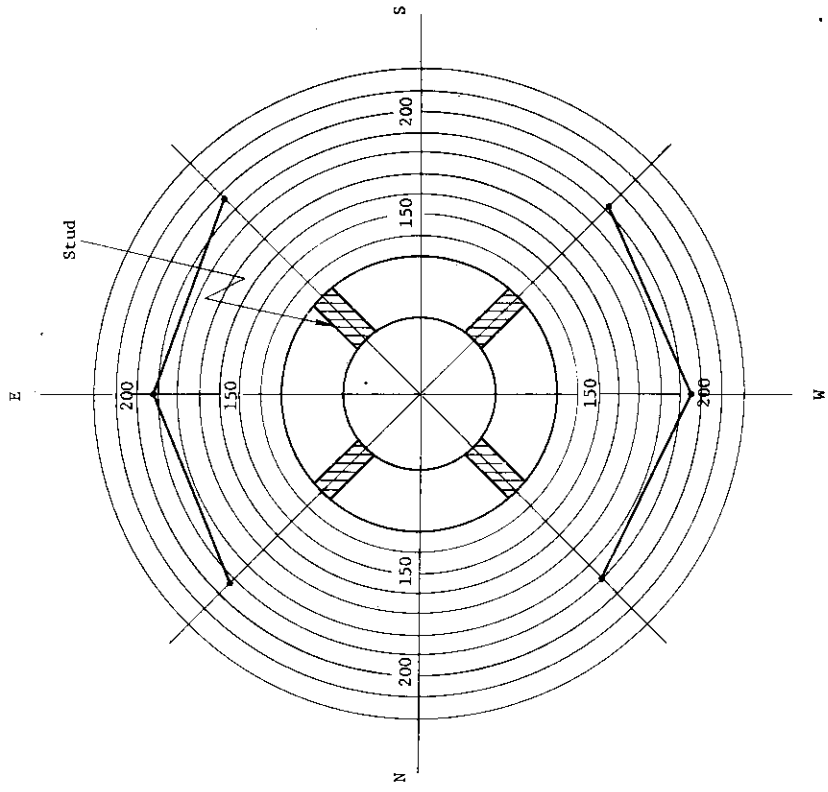

Fig. 6.15 Stud of upper and perpendicular part of the hot gas duct at C31 side

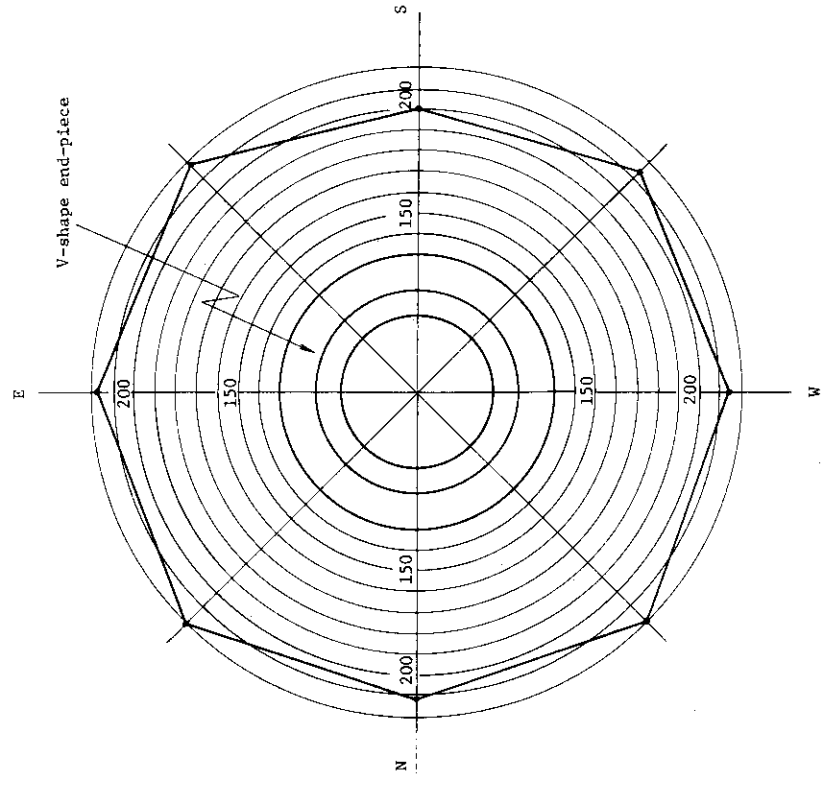

Fig. 6.14 V-shape end-piece of lower and perpendicular part of the hot gas duct at C31 side

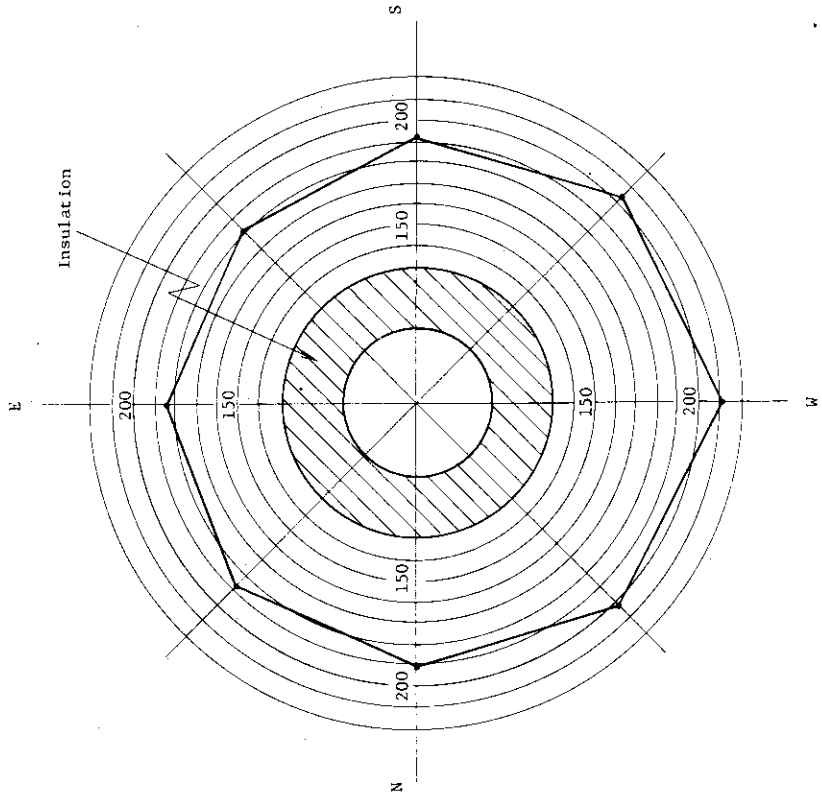

Fig. 6.17 Fourth elbow of the hot gas duct

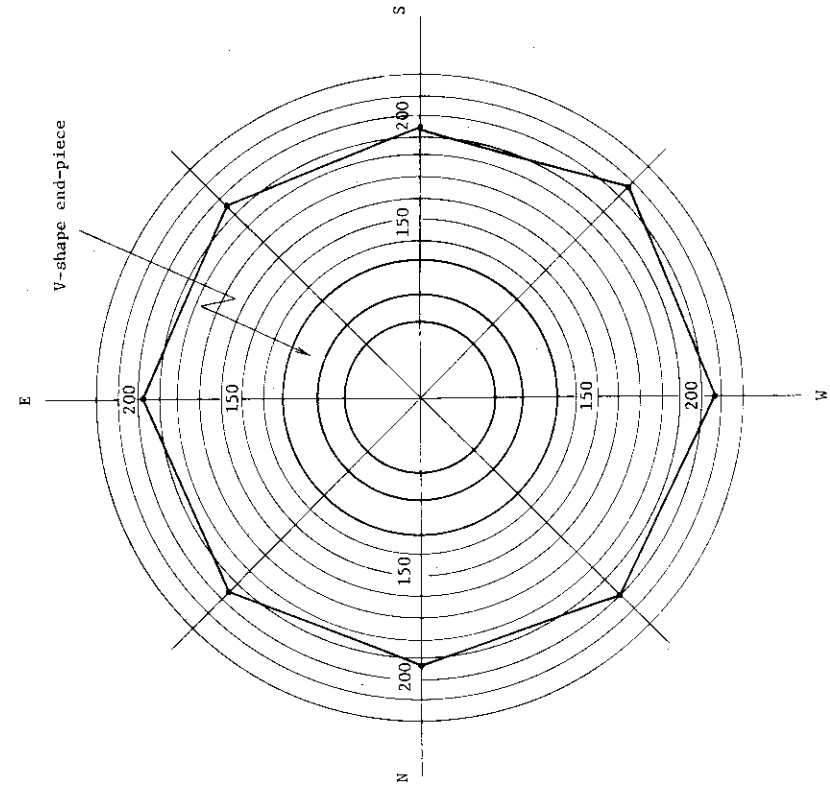

Fig. 6.16 V-shape end-piece of upper and perpendicular part of the hot gas duct at C31 side

(2) Measurement with a radiative thermometer

(2)-1 Radiative thermometer

(a) Principle

Thermal radiation is defined by the following equation which is known as Stefan-Bolzman law.

$$E = \varepsilon\sigma T^4$$

E : emissive power per unit area and unit time

ε : emissivity

σ : Stefan-Bolzman constant

T : absolute temperature

If emissivity is assumed to be constant, emissive power is determined only by temperature. A radiative thermometer is made to obtain temperature and temperature distribution by measuring emissive power.

The radiative thermometer is very useful to measure temperature distribution, especially to detect hot sopts.

(b) Specification

Temperature range	:	-40 ∿ 2000°C
Scope	:	±20° vertical
		±25° horizontal
Focus	:	20cm ∿ ∞
Lens material	:	Germanium

(2)-2 Results of temperature distribution of the hot gas duct

Figures 6.18∿6.35 show the temperature distribution of the hot gas duct measured by a radiative thermometer.

No hot spot was detected at the surface of the pressure tube.

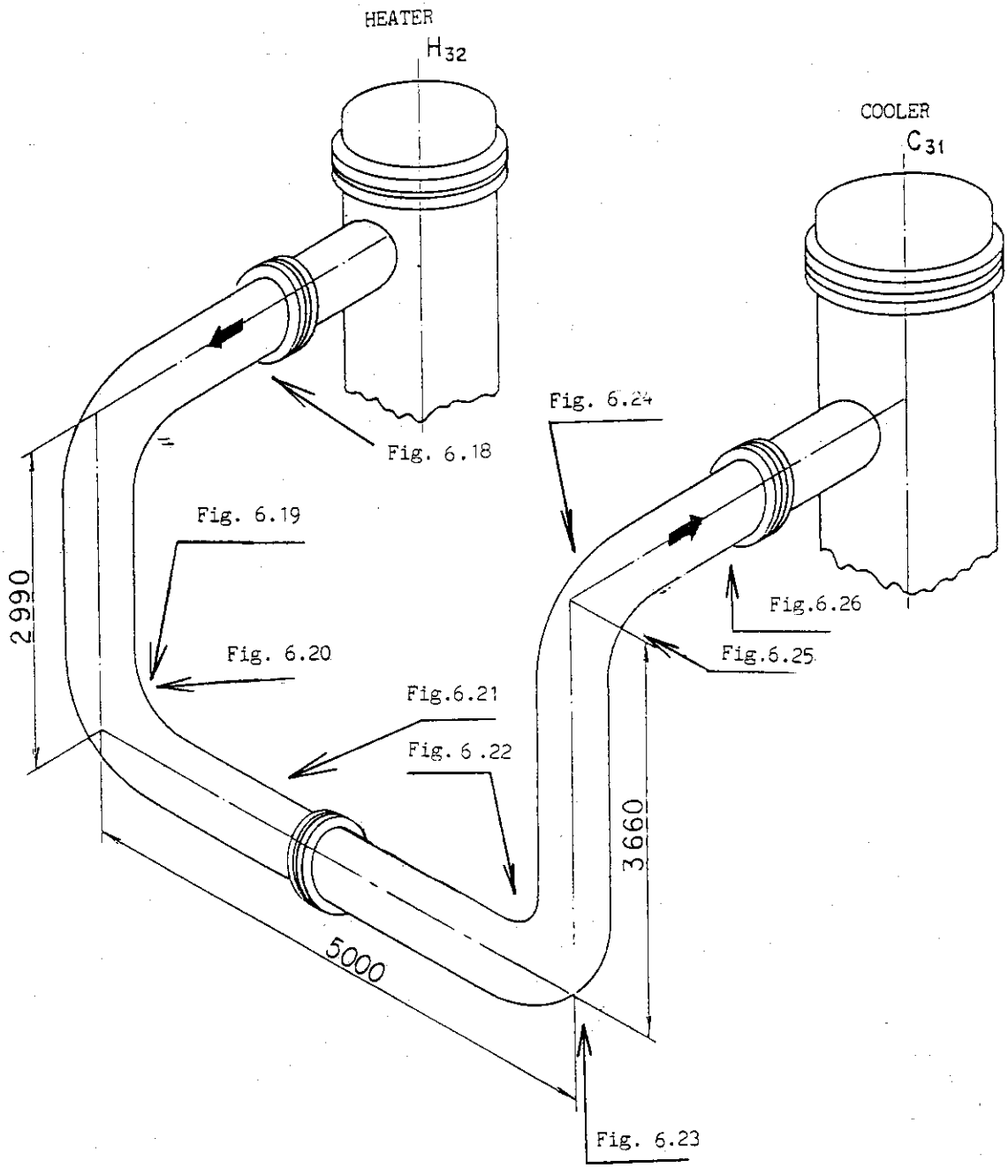

Measuring location of the hot gas duct (test operation)

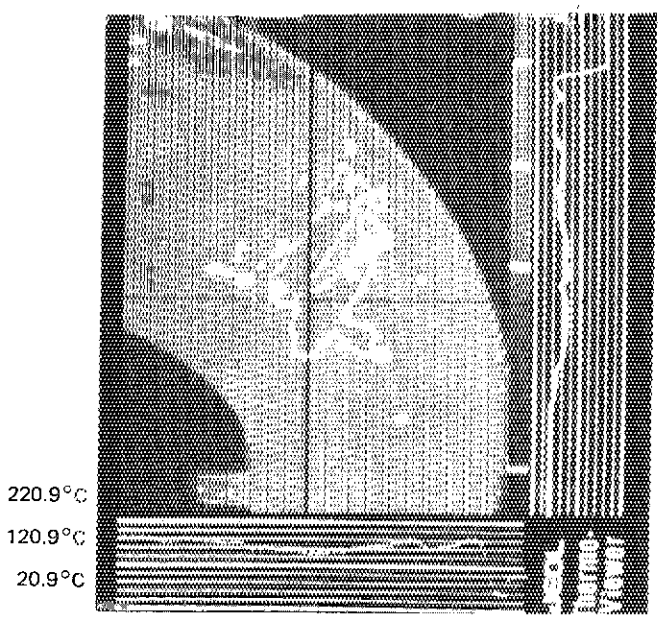

Fig. 6.20

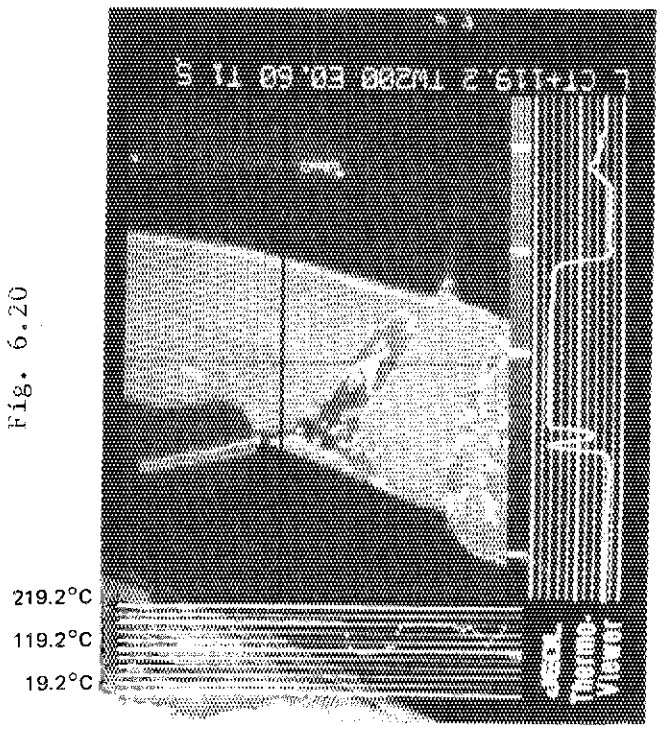

Fig. 6.21

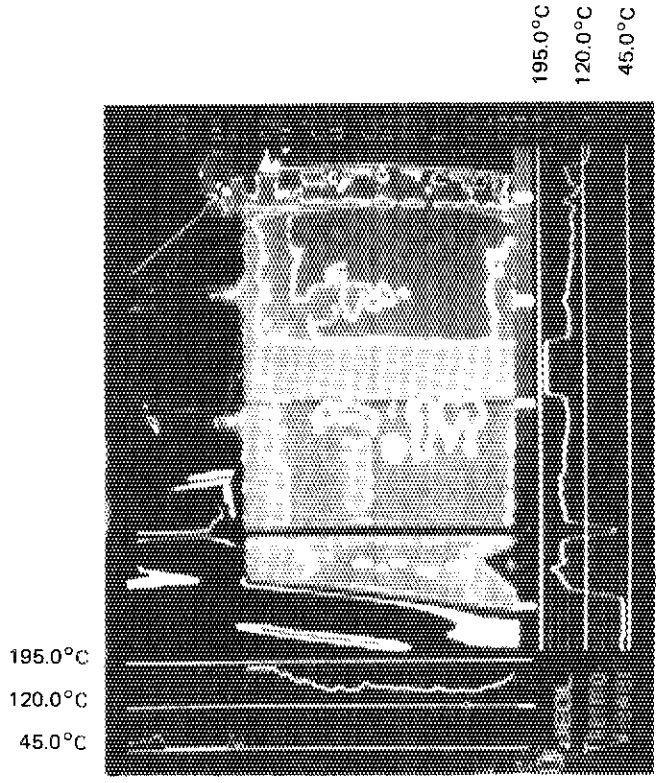

Fig. 6.18

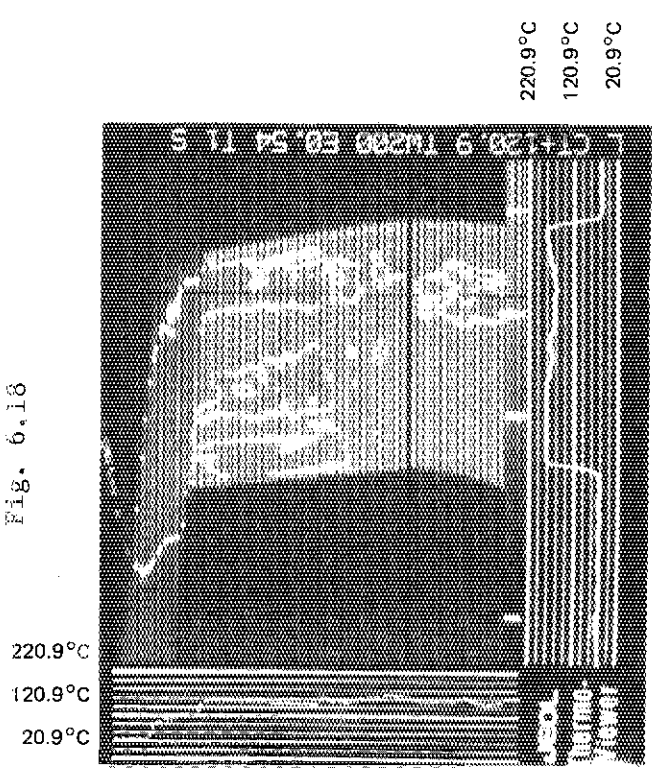

Fig. 6.19

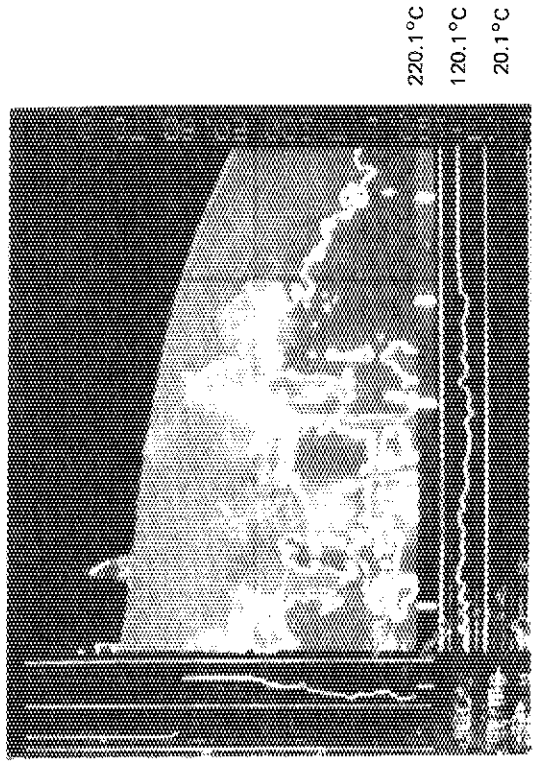

Fig. 6.24

Fig. 6.25

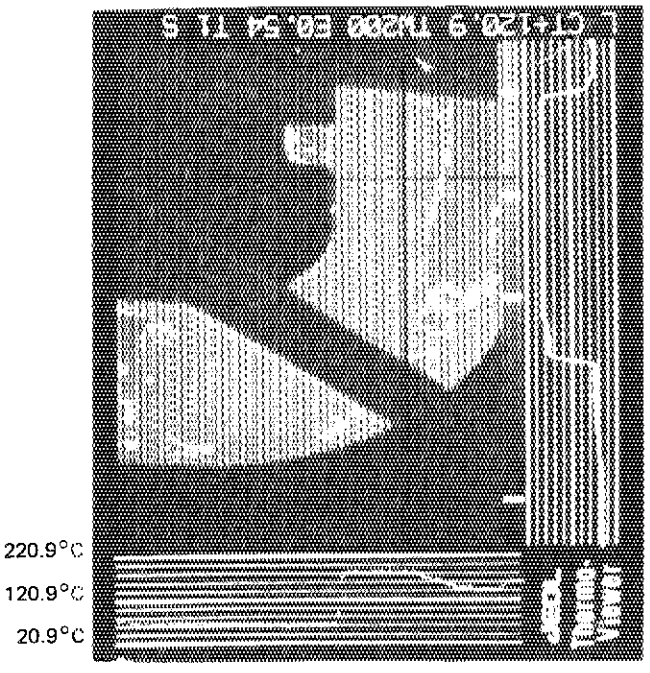

Fig. 6.22

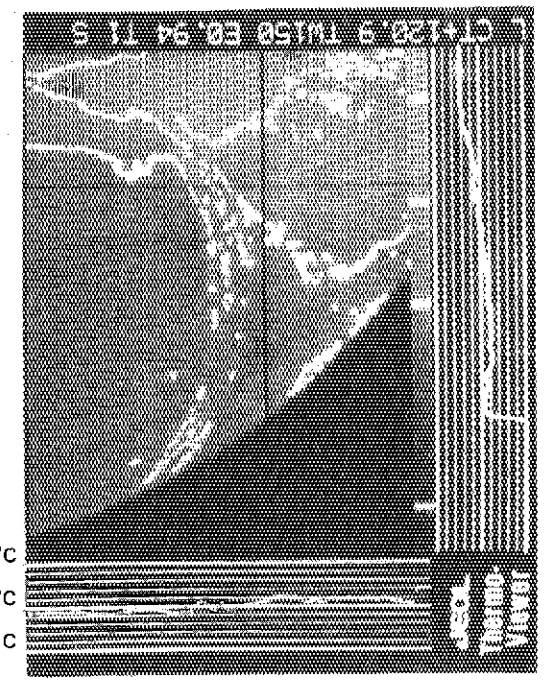

Fig. 6.23

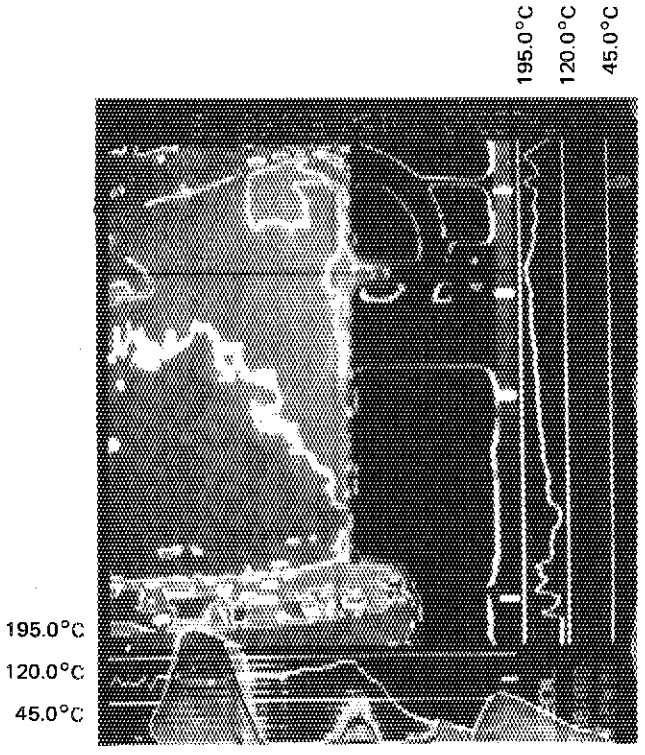

Fig. 6.26

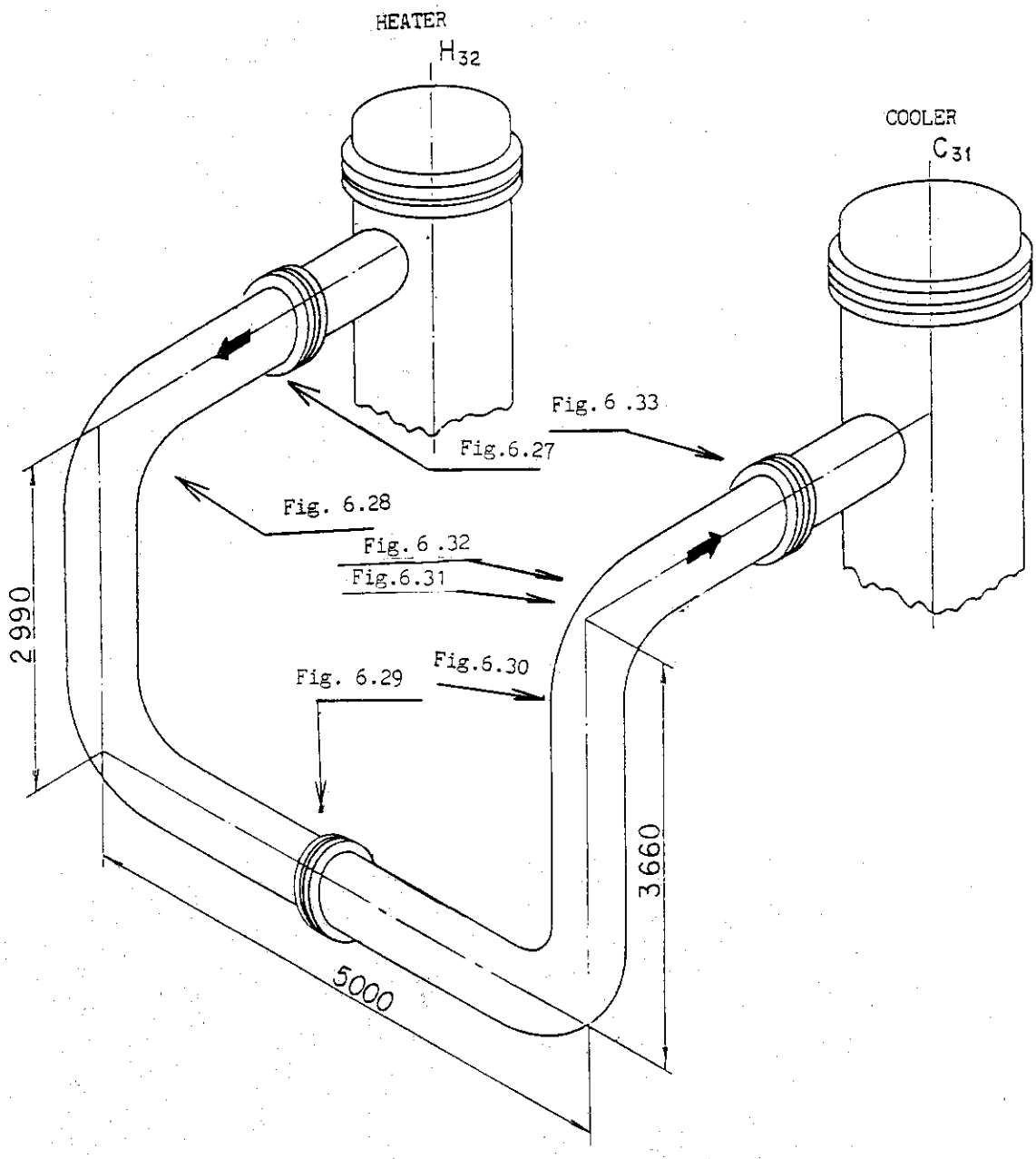

Measuring location of the hot gas duct (NO.1 cycle test)

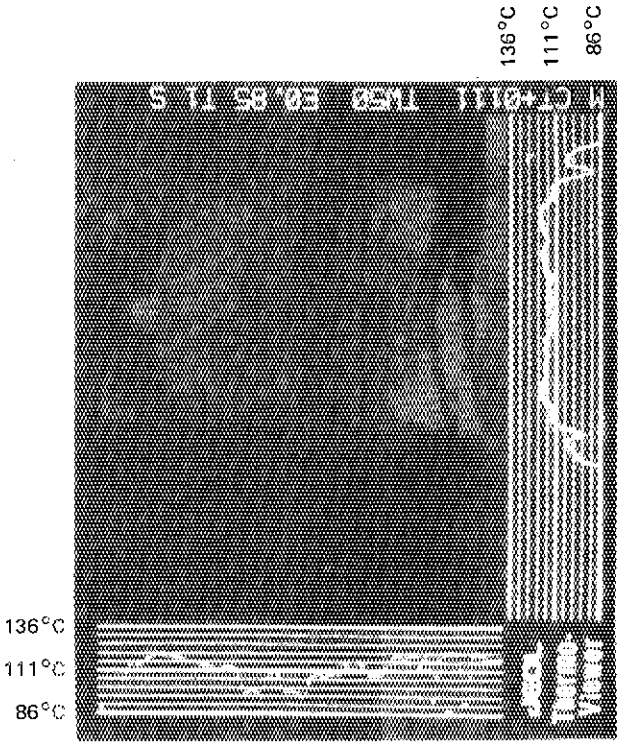

Fig. 6.29

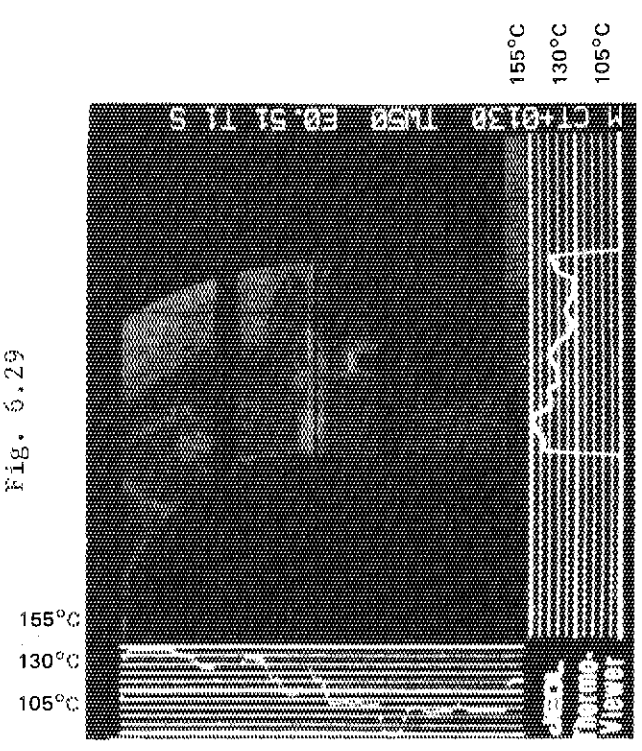

Fig. 6.30

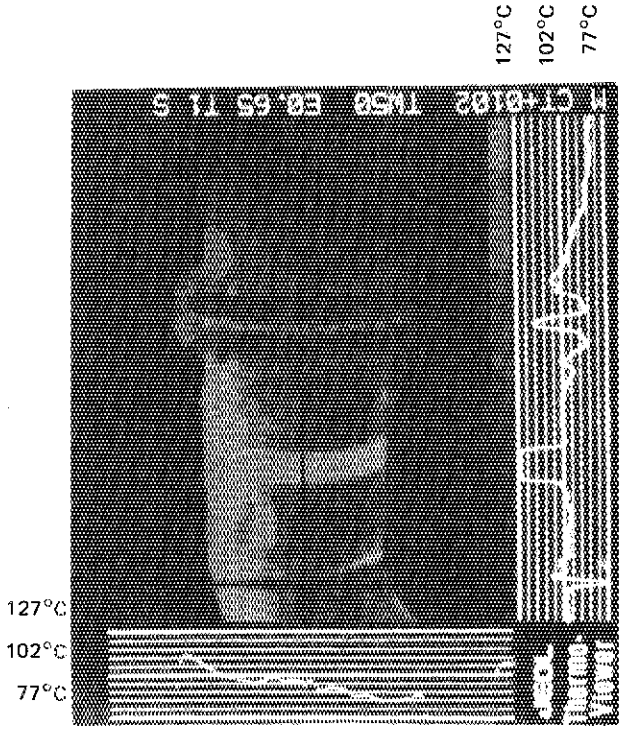

Fig. 6.27

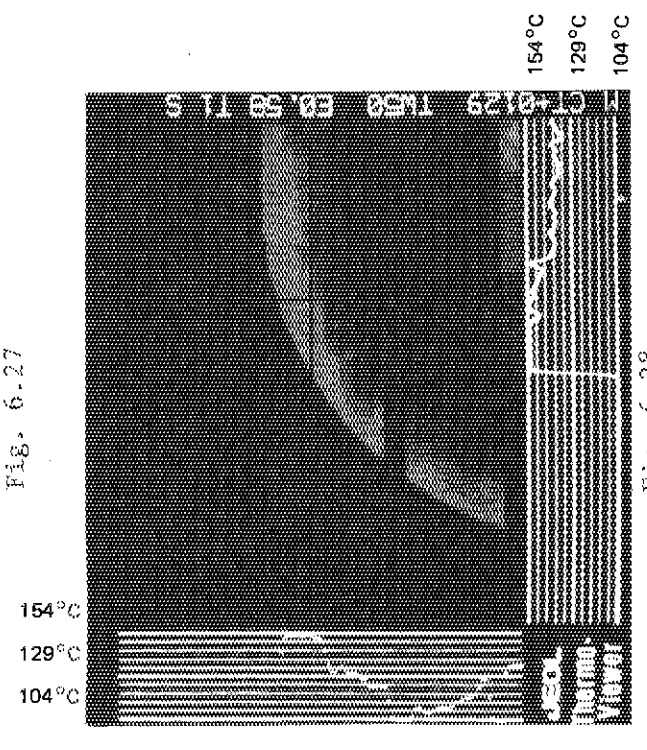

Fig. 6.28

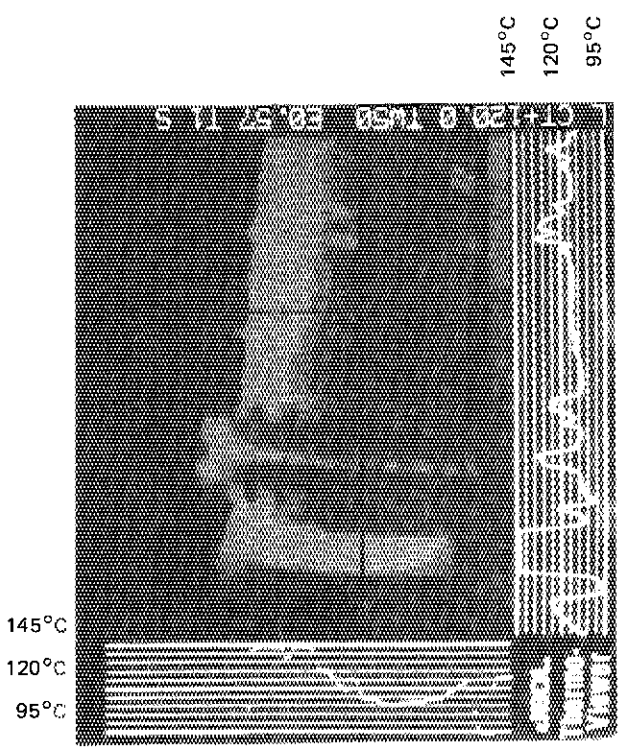

Fig. 6.33

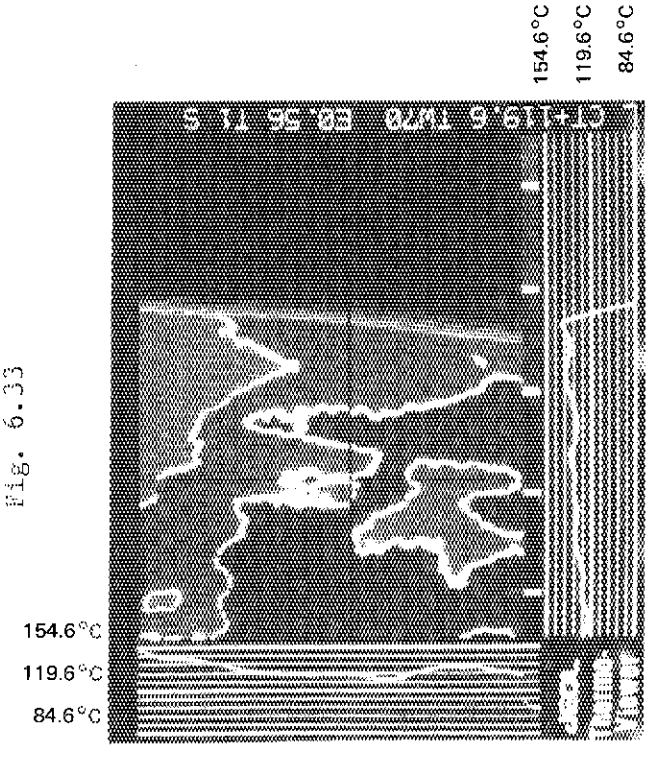

Fig. 6.34

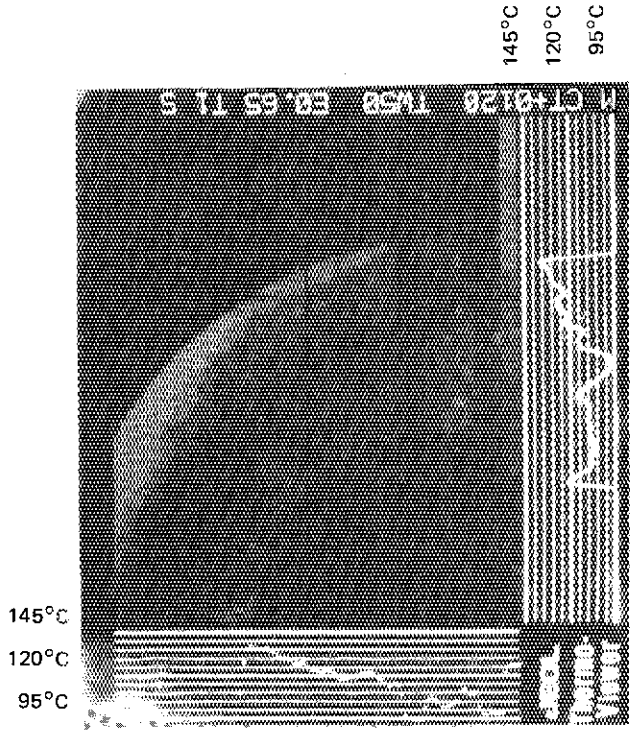

Fig. 6.31

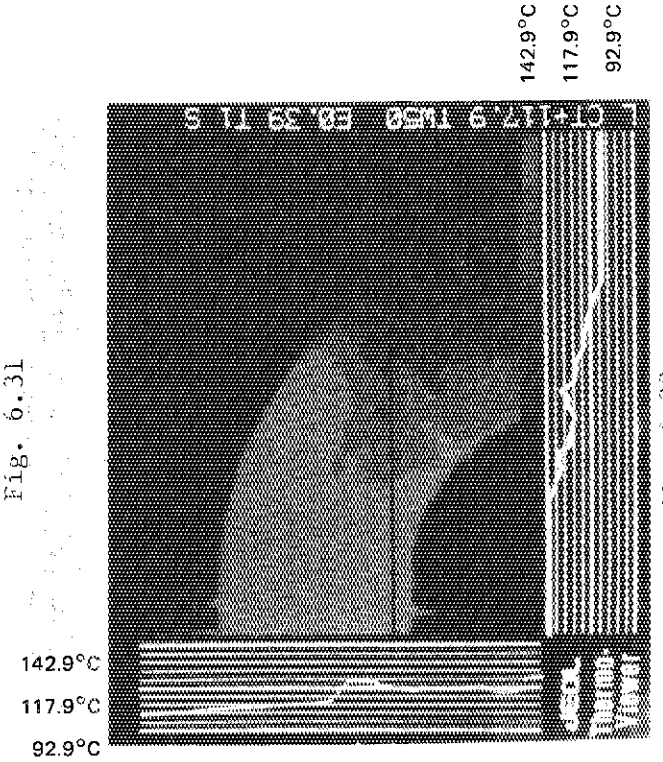

Fig. 6.32

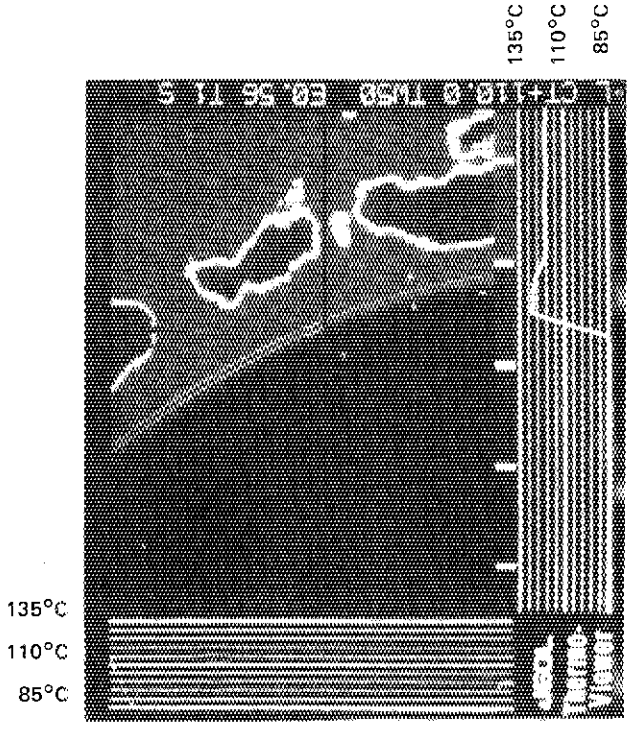

Fig. 6.35

7. Measurement of heat flux at the surface of the pressure tube with a heat flux meter

(1) Principle of measurement

As shown in Fig. 7.1, temperature difference is generated between both sides of the heat resistance material, when heat flows across the material.

By measuring this temperature difference with two thermocouples fixed on the both surfaces of a heat residence material, a standard relationship between the temperature difference and heat flux is to be established.

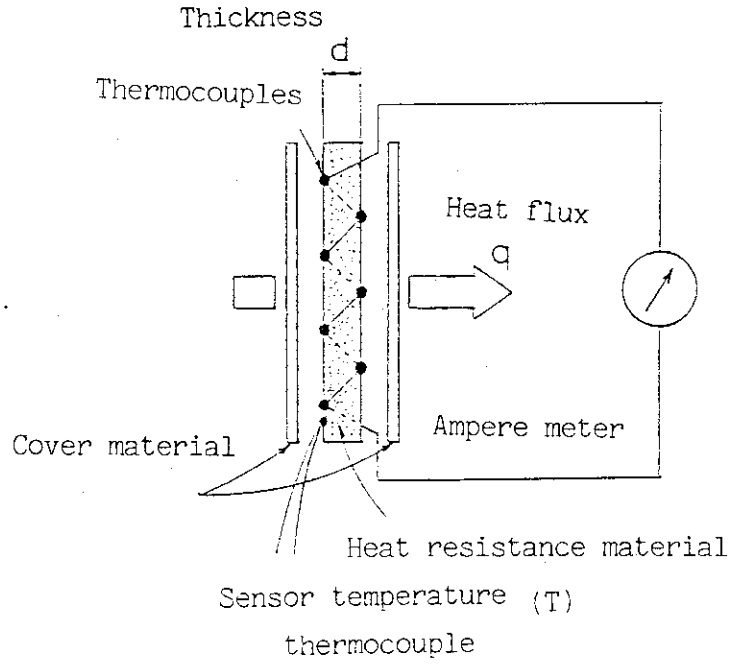

Fig. 7.1 Principle of measurement

Main specification of the heat flux meter used is as follows;

Heat resistance material	:	silicon rubber
Measuring range	:	10 ∿ 3000 kcal/m^{2}h
Accuracy	:	±0.4 kcal/m^{2}h (in the region below 20 kcal/m^{2}h)
	:	±2% (within the range of 20 ∿ 100 kcal/m^{2}h)
	:	±1% (in the region over 100 kcal/m^{2}h)

The results of preliminary measurement with a heat flux meter are a little bit higher than the calculated values. (The results and method of calculation are described in Appendix 2) This might be open to the further investigation.

Fig. 7.2 Measuring points at the surface of the pressure tube

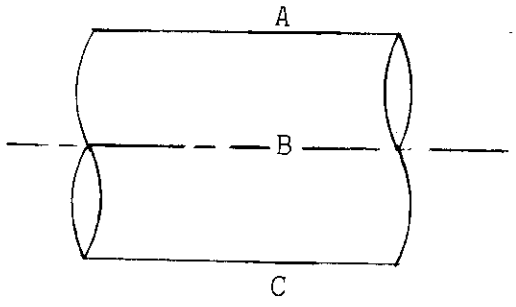

Table 7.1 Heat fluxes obtained with a heat flux meter and calculated heat transfer coefficients

	Gas temperature (^{o}C)	Surface temperature of the pressure tube (^{o}C)	Heat flux (kcal/m^{2}h)	Heat transfer coefficient (kcal/m^{2}h^{o}C)
A	800	125	1860	17.7
B	800	143	1560	12.7
C	800	157	2200	16.1

room temperature : 20^{o}C

8. Conclusion

The following conclusions were obtained;

(1) The average radial temperature distribution within the insulation layer were almost linear.

(2) The maximum temperature of the pressure tube was about 230°C. It was below the design temperature of the pressure tube (350°C). Temperature distribution measured by fixed thermocouples and a contacting thermometer indicated that the temperature at the bottom of the pressure tube was 30 ∿ 70°C higher than that at the top. No significant hot spots, however, were detected by fixed thermocouples, a contacting thermometer and a radiative thermometer.

(3) Effective thermal conductivity of the insulation layer was estimated to be 0.4 ∿ 0.49 kcal/mh°C at 590°C of the average temperature of the insulation, under the assumption that heat transfer coefficient of air around the hot gas duct was about 12 kcal/m^2h°C.

Reference

(1) T. Umeda, T. Nishidono, IHI Technical Report Vol.20, No.6 (1980).

Appendix 1 Measured data of the hot gas duct

Table A1-1 Measured data of the hot gas duct (test operation).

Date		3/16	3/16	3/17	3/18	3/18	3/18	3/19	3/24	3/26	3/28
Time		0:00	21:32	14:33	9:00	14:16	19:46	7:02	16:30	14:00	14:00
Helium Gas Temperature (Heater H_{32} Outlet) (°C)		320.7	494.2	573.1	699.4	801.0	903.7	1000.0	1000.0	880.0	1000.0
Flow Rate (kg/s)		2.810	2.798	2.800	2.802	2.803	2.797	2.800	2.799	4.004	0.400
Gas Pressure (kg/cm^2g) (Heater H_{32} Outlet)		39.30	39.52	39.67	39.97	39.97	39.97	39.97	40.00	40.00	40.00
Insulation Temperature (H_{32} Outlet) (°C) ①	1	150.0	227.5	262.4	319.8	365.9	409.7	454.2	467.0	405.4	458.3
	2								766.7	669.2	758.0
	3	318.4	488.4	567.1	692.5	792.5	894.4	990.4	991.6	876.0	997.3
	4								760.7	664.8	751.6
	5								536.8	417.0	559.4
	6								776.6	677.6	768.4
	7	143.9	217.8	252.7	310.1	357.6	402.6	451.9	464.6	398.3	459.4
Insulation Temperature (C_{31} Inlet) (°C) ⑥	8								461.2	400.7	440.3
	9								763.0	667.1	737.9
	10								991.6	875.2	959.4
	11								760.1	661.0	735.2
	12								483.5	417.1	463.0
	13								764.4	669.9	735.2
	14								454.1	392.4	434.6
V-shape end-piece Temperature (H_{32} Outlet) (°C) ②	15	65.3	96.2	108.1	131.9	151.3	168.8	183.5	200.8	155.8	203.8
	16	141.5	214.2	249.0	306.5	350.5	394.3	440.2	451.8	390.1	448.7
	17								941.9	817.3	937.8
	18								553.8	451.4	565.3
	19								536.1	427.9	551.5
V-shape end-piece Temperature (C_{31} Inlet) (°C) ⑤	20								280.8	241.8	272.2
	21								567.4	498.4	552.7
	22								939.6	831.3	911.1
	23								548.6	471.2	526.9
	24								581.1	504.5	560.0
Pressure Tube (H_{32} Outlet) (°C) ③	25	59.2	85.2	97.1	115.9	136.7	149.2	165.1	166.0	140.0	166.2
	26								181.0	150.0	171.5
	27	62.9	91.3	97.1	124.4	145.2	160.2	176.2	195.0	158.0	181.4
	28								168.0	148.0	186.5
	29	69.0	97.6	106.9	134.3	157.6	175.0	187.2	215.0	166.0	198.6
	30								178.0	170.0	196.2
Pressure Tube (C_{31} Inlet) (°C) ④	31	59.2	86.4	97.1	117.1	136.7	149.2	165.1	178.0	148.0	169.2
	32								170.0	150.0	170.4
	33	60.4	88.8	99.6	119.5	141.6	154.1	168.8	186.0	150.0	175.3
	34								180.0	148.0	175.4
	35	69.0	97.4	106.9	134.3	156.2	171.2	186.0	215.0	168.0	198.6
	36								192.0	170.0	183.4

Table A1-2 Measured data of the hot gas duct (NO.1 cycle test).

Date		7/1	7/1	7/1	7/2	7/3	7/5	7/6
Time		11:32	15:02	22:31	19:47	19:40	9:02	9:16
Helium Gas Temperature (Heater H_{32} Outlet) (^{o}C)		317.3	437.7	582.8	699.4	799.9	896.9	997.4
Flow Rate (kg/s)		1.304	1.302	1.303	1.506	1.502	1.505	1.505
Gas Pressure (kg/cm^2g) (Heater H_{32} Outlet)		27.97	30.00	31.95	34.35	36.00	39.75	39.75
Insulation Temperature (H_{32} Outlet) (^{o}C) ①	1	147.5	195.4	262.3	317.5	368.5	414.4	462.6
	2							
	3	314.6	433.9	575.2	691.4	791.6	888.2	987.8
	4	232.1	318.2	430.2	521.9	600.6	679.7	760.9
	5							
	6							
	7	143.8	190.4	257.4	313.8	365.0	413.2	462.6
Insulation Temperature (C_{31} Inlet) (^{o}C) ⑥	8							
	9							
	10							
	11							
	12							
	13							
	14							
V-shape end-piece Temperature (H_{32} Outlet) (^{o}C) ②	15	66.4	81.1	110.5	133.2	159.1	179.9	202.2
	16	141.2	186.7	252.5	307.8	358.0	403.8	450.8
	17							
	18							
	19							
V-shape end-piece Temperature (C_{31} Inlet) (^{o}C) ⑤	20							
	21							
	22							
	23							
	24							
Pressure Tube (H_{32} Outlet) (^{o}C) ③	25	64.0	75.0	99.4	113.5	140.6	156.5	173.8
	26							
	27	66.4	80.0	106.8	124.6	151.7	168.8	188.4
	28							
	29	72.5	86.0	117.8	141.8	173.9	192.1	219.1
	30							
Pressure Tube (C_{31} Inlet) (^{o}C) ④	31	64.0	76.2	100.7	111.1	139.4	154.1	171.2
	32							
	33	65.2	77.4	104.3	119.6	145.6	161.4	179.9
	34							
	35	73.8	86.0	117.8	140.5	172.6	190.0	216.7
	36							

Table A1-3 Measured data of the hot gas duct (NO.2 cycle test).

Date		10/7	10/8	10/9	10/10
Time		0:02	0:46	0:46	1:02
Helium Gas Temperature (Heater H_{32} Outlet)(°C)		699.1	801.1	899.8	998.7
Flow Rate (kg/s)		4.002	4.008	2.792	2.799
Gas Pressure (kg/cm^2g) (Heater H_{32} Outlet)		39.97	39.97	40.05	39.97
Insulation Temperature (H_{32} Outlet) (°C) ①	1	312.1	366.2	413.9	461.4
	2				
	3	693.4	796.6	892.6	991.8
	4	516.7	600.9	680.4	762.1
	5				
	6				
	7	302.4	359.2	411.5	460.2
Insulation Temperature (C_{31} Inlet) (°C) ⑥	8				
	9				
	10				
	11				
	12				
	13				
	14				
V-shape end-piece Temperature (H_{32} Outlet) (°C) ②	15	108.1	137.0	172.0	193.3
	16	295.2	352.1	403.3	450.8
	17				
	18				
	19				
V-shape end-piece Temperature (C_{31} Inlet) (°C) ⑤	20				
	21				
	22				
	23				
	24				
Pressure Tube (H_{32} Outlet) (°C) ③	25	105.7	134.5	156.0	171.2
	26				
	27	115.6	145.6	168.4	187.2
	28				
	29	125.3	162.8	192.8	215.5
	30				
Pressure Tube (C_{31} Inlet) (°C) ④	31	106.9	134.5	154.8	170.0
	32				
	33	110.6	140.6	162.1	177.4
	34				
	35	124.1	162.8	192.8	214.3
	36				

Appendix 2. Calculating method of the effective thermal conductivity

(1) Effective thermal conductivity

The effective thermal conductivity is defined by the following equation.

$$\lambda = \frac{Q}{2\pi} \ln \frac{r_2}{r_1} \frac{1}{(\theta_1 - \theta_2)} \qquad (1)$$

λ : effective thermal conductivity
Q : heat flux per unit length
r_2 : outer radius of the pressure tube
r_1 : inner radius of the pressute tube
θ_2 : average temperature of the pressure tube
θ_1 : temperature of the liner

(2) Heat flux per unit length

The heat flux per unit length is difined as follows.

$$Q = \alpha\pi D \ (\theta_2 - \theta_a) \qquad (2)$$

Q : heat flux per unit length
α : heat transfer coefficient at the surface of the pressure tube
D : outer diameter of the pressure tube
θ_a : room temperature
θ_2 : average temperature of the pressure tube

Room temperature (θ_a) is assumed to be 20°C, because the thermocouples in the building indicated approximately 20°C during the course of the operations (NO.1 and NO.2 cycle tests)

(3) Heat transfer coefficient at the surface of the pressure tube

The heat transfer coefficient at the surface of the pressure tube (α) is defined as the sum of the coefficients by thermal radiation (α_r) and free convection (α_f).

$$\alpha = \alpha_r + \alpha_f \qquad (3)$$

In order to obtain the coefficient by free convection (α_f) around

the hot gas duct, the following equation (Jacob's formula) is used.

$$\alpha_f = 0.13\ Ra^{1/3}\frac{\lambda}{D} \qquad (4)$$

As for the coefficient by thermal radiation (α_r), we used the following Stefan-Bolzman's equation.

$$\alpha_r = 4.88\ \varepsilon\ \frac{(\frac{T_2}{100})^4 - (\frac{293}{100})^4}{(T_2 - 293)} \qquad (5)$$

Ra : Rayleigh number

ε : emissivity

D : outer diameter of the pressure tube

T_2 : average absolute temperature of the pressure tube

λ : thermal conductivity of air

(4) Calculated effective thermal conductivities

Table A2-1 Effective thermal conductivity (test operation)

Date	3/16	3/16	3/17	3/18	3/18	3/19	3/19
Time	0:00	21:32	14:33	9:00	14:16	17:46	7:02
Helium gas temperature(°C)	320.7	494.2	573.1	699.4	801.0	903.7	1000.
Temperature of the pressure tube(°C)	63.26	91.3	100.8	124.3	145.7	159.8	174.7
Temperature of the liner(°C)	318.4	489.5	569.5	693.7	795.0	898.0	993.9
Average temperature of the insulation(°C)	190.8	290.4	355.1	409.0	470.3	528.9	584.3
Heat transfer coefficient(kcal/m^{2}h°C)	7.69	9.12	9.58	10.28	10.92	11.39	11.90
Heat flux per unit length (kcal/mh)	690.2	1349.1	1605.4	2223.2	2847.2	3303.6	3819.4
Effective thermal conductivity(kcal/mh°C)	.237	.297	.300	.342	.384	.392	.408

Table A2-2 Effective thermal conductivity (NO.1 cycle test)

Date	7/1	7/1	7/1	7/2	7/3	7/5	7/6
Time	11:32	15:02	22:31	19:47	19:40	9:02	9:16
Helium gas temperature (°C)	316.4	438.0	583.4	699.0	799.4	897.0	999.0
Temperature of the pressure tube (°C)	67.62	80.1	107.8	125.2	154.0	170.6	191.5
Temperature of the liner (°C)	314.6	433.9	575.2	691.4	791.6	888.2	987.8
Average temperature of the insulation(°C)	191.1	257.0	341.5	408.3	472.8	529.4	589.7
Heat tansfer coefficient (kcal/m^{2}h°C)	7.91	8.55	9.79	10.31	11.19	11.76	12.49
Heat flux per unit length (kcal/mh)	781.5	1066.1	1783.3	2250.3	3110.9	3674.4	4444.1
Effective thermal conductivity(kcal/mh°C)	.277	.264	.334	.348	.439	.448	.489

Table A2-3 Effective thermal conductivity (NO.2 cycle test)

Date	10/7	10/8	10/9	10/9
Time	0:02	0:46	0:46	1:02
Helium gas temperature (°C)	699.0	798.0	898.4	999.0
Temperature of the pressure tube (°C)	114.7	146.8	171.2	189.3
Temperature of the liner (°C)	693.4	796.6	892.6	991.8
Average temperature of the insulation(°C)	404.1	471.7	531.9	590.6
Heat transfer coefficient (kcal/m^{2}h°C)	10.00	10.95	11.78	12.41
Heat flux per unit length (kcal/mh)	1964.8	2880.6	3695.3	4359.0
Effective thermal conductivity(kcal/mh°C)	.297	.388	.448	.476

Appendix 3. Comparison with the measured and calculated results of radial temperature distribution in the insulation

Radial temperature distribution is calculated by using the following equation.

(1) Assuming that thermal conductivity of the insulation is constant.

$$Q = -\lambda 2\pi r \frac{dt}{dr} \qquad (1)$$

$$t = -\frac{Q}{2\pi\lambda} \ln \left(\frac{r}{r_0}\right) + t_0 \qquad (2)$$

Q : heat flux per unit length
λ : thermal conductivity of the insulation
t : temperature
r : radius
r_0 : radius of the liner
t_0 : temperature of the liner

(2) Assuming that thermal conductivity is a linear function of temperature.

Thermal conductivity of insulation derived from the measured results of Fig. A3-1 is expressed as follows.

$$\lambda = 0.168 + 4.53 \times 10^{-4} t \qquad (3)$$

Radial temperature distribution of the following equation (4) is obtained by substituting equation (3) into equation (2).

$$Q = -(0.168 + 4.53 \times 10^{-4} t) 2\pi r \frac{dt}{dr}$$

$$\int_{t_0}^{t} -(0.168 + 4.53 \times 10^{-4} t)\, dt = \frac{Q}{2\pi} \int_{r_0}^{r} \frac{1}{r}\, dr$$

$$t = \frac{-0.168 + \sqrt{0.168^2 - 2 \cdot 4.53 \times 10^{-4} \cdot \left(-\frac{4.53}{2} \times 10^{-4} t_0^2 - 0.168 t_0 + \frac{Q}{2\pi} \ln\left(\frac{r}{r_0}\right)\right)}}{4.53 \times 10^{-4}} \qquad (4)$$

Figures A3-2, A3-4 show the comparison with the measured and

calculated results. If linear dependency of temperature on thermal conductivity is assumed, the measured results approximately agreed with the calculated values.

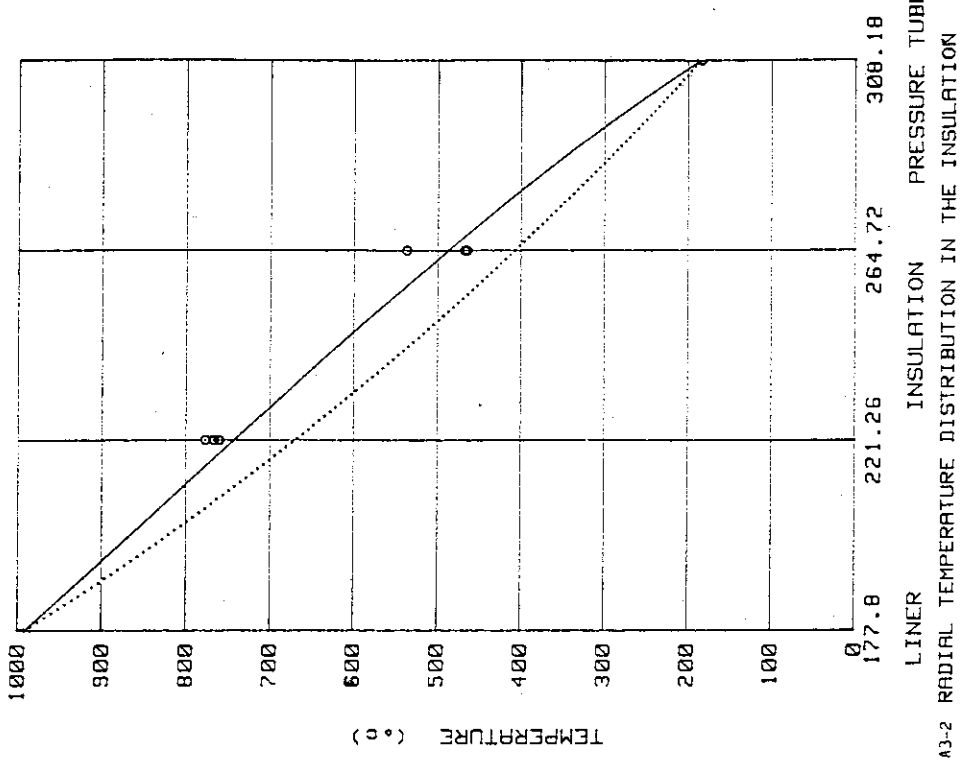

Fig. A3-2 RADIAL TEMPERATURE DISTRIBUTION IN THE INSULATION

o measured temperature

..... calculation (effective thermal conductivity is constant)

— calculation (effective thermal conductivity is changed linearly with temperature)

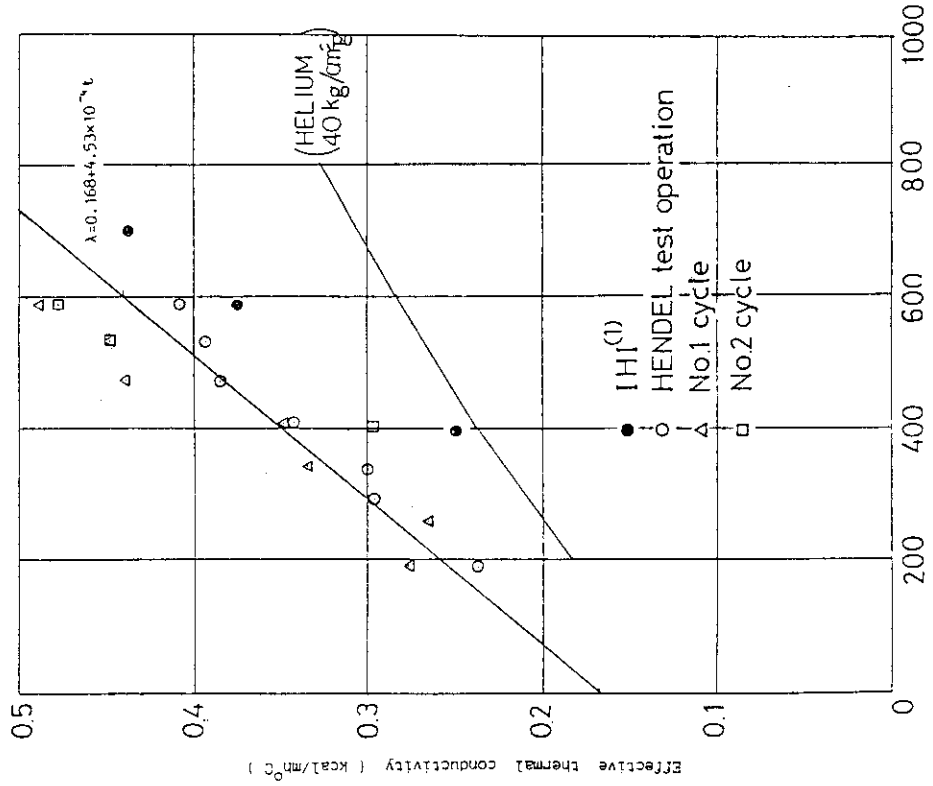

Fig. A3-1 Effective thermal conductivity of the hot gas duct

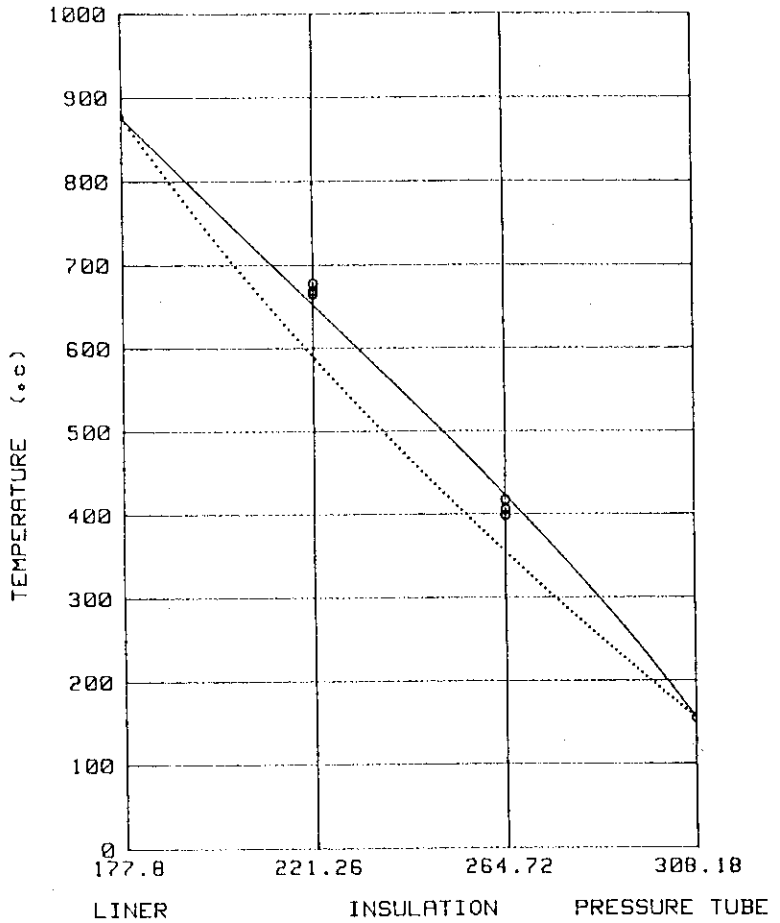

Fig. A3-3 RADIAL TEMPERATURE DISTRIBUTION IN THE INSULATION

o measured temperature

····· calculation (effective thermal conductivity is constant)

—— calculation (effective thermal conductivity is changed linearly with temperature)

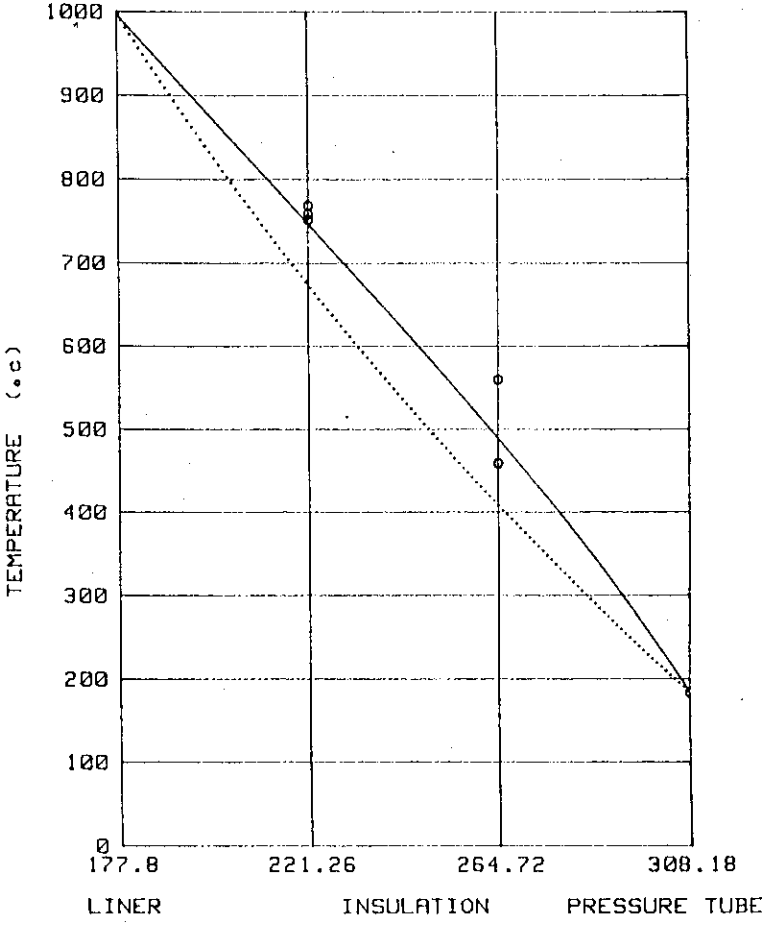

Fig. A3-4 RADIAL TEMPERATURE DISTRIBUTION IN THE INSULATION

o measured temperature

····· calculation (effective thermal conductivity is constant)

—— calculation (effective thermal conductivity is changed linearly with temperature)